

# Fundamental and approximate symmetries, parity violation and tunneling in chiral and achiral molecules

**Martin Quack\*, Georg Seyfang, and Gunther Wichmann**

Physical Chemistry, ETH Zürich, CH-8093 Zürich, Switzerland

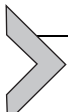
\*Corresponding author: e-mail address: martin@quack.ch

## Contents

1. Introduction	52
2. Basic concepts of symmetry breakings, approximate constants of the motion and a survey of time scales for molecular processes	54
3. Time dependence of exotic superpositions and the molecular quantum chameleon	65
3.1 Elementary scheme for intramolecular coupling and symmetry breaking	65
3.2 Violation of nuclear spin symmetry and the superposition of nuclear spin isomers	71
3.3 Mixing and superposition of structural isomers: The molecular quantum switch	78
3.4 Relaxation processes in multistate systems at high densities of states	81
4. The experimental approach toward parity violation in chiral molecules	82
5. Concluding remarks on theory, experiment, and future possibilities	89
Acknowledgments	92
References	92

## Abstract

We introduce the basic concepts of symmetry breakings and approximate constants of the motion in relation to time scales for molecular primary processes from yoctoseconds to seconds and extending to the age of the universe. We then discuss the concepts for the experimental approach to study these processes of molecular quantum dynamics by high-resolution spectroscopy and the basic scheme for control of symmetries and the observation of the evolution of approximate constants of the motion by generating “exotic superposition isomers.” We illustrate the results from our theoretical and experimental work with emphasis on the conservation and violation of nuclear spin symmetry and parity violation in chiral and achiral molecules.



## 1. Introduction

Symmetry and asymmetry are concepts which are used in a wide range of contexts from the fundamental sciences, mathematics, physics, chemistry, and biology to the arts, music, and architecture.<sup>1</sup> If asymmetries are small, one may still introduce the concept of approximate symmetries. Symmetries in physics and chemistry can be associated with constants of the motion, and correspondingly approximate symmetries with approximate constants of the motion. Particularly interesting approximate molecular symmetries lead to the approximate conservation of nuclear spin symmetry and parity in spectroscopy and kinetics.<sup>2–4</sup> In the present article we shall start with an outline of how symmetries can be applied to the understanding of the time scales in fundamental kinetic primary processes. We shall briefly discuss our approach to derive molecular quantum dynamics from high-resolution spectroscopy and illustrate it with some selected examples from our research including results on intramolecular energy flow and molecular tunneling and tunneling switching phenomena in free molecules and under excitation with coherent time-dependent electromagnetic fields. The control of symmetry by external fields is of particular interest. We introduce the concepts of our experimental approach to prepare interesting non-classical states of well-defined initial symmetry and observe the subsequent evolution of the approximate symmetry property or “constant of the motion” with time to study fundamental primary processes in general, quantum molecular switches for quantum technology, and molecular parity violation, in particular. The time-dependent process of parity change connects molecular physics with the standard model of particle physics (SMPP) and we shall report about the current status of our project on this topic.

The experimental investigation of time-dependent molecular processes notably by spectroscopic observation has a long and rich history, starting with Wilhelmy’s investigation in 1850 of the “inversion” of sugar by means of the study of time-dependent optical activity. For the kinetics of the solution of sugar containing also an acid he formulated and analyzed a pseudo-first order rate law of what turned out to be also the first quantitative kinetic analysis of homogeneous catalysis.<sup>5</sup> Reaction times were then conveniently measured by ordinary clocks on quite suitable time scales of much more than seconds. A century later, formerly “immeasurably fast” reactions on the microsecond to nanosecond time scales were investigated by time resolved techniques developed by Eigen<sup>6,7</sup> and Norrish and Porter<sup>8</sup> as well as by shock wave techniques.<sup>9,10</sup> The picosecond and femtosecond ranges were

made accessible in the time from 1970 to 1990<sup>8,11,12</sup> and today's short time frontier is attosecond kinetics and spectroscopy<sup>13–15</sup> (we do not claim any completeness in this short history, see also Refs. 16–29 for various aspects and further references cited therein).

In parallel to experiments in the 20th century, quantum theory for kinetic primary processes was developed with the time-dependent Schrödinger equation<sup>30–34</sup> and the Heisenberg equations of motion.<sup>35–37</sup> Slow tunneling processes<sup>38–40</sup> and fast exponential decay processes<sup>41,42</sup> were analyzed by quantitative theory (see the reviews in Refs. 25–29, 43–45).

Starting from about 1980 we developed an experimental approach based on molecular spectroscopy with high frequency resolution, but low time resolution, even stationary, in combination with a quantum theoretical analysis, which allows for covering essentially all time scales from the yoctoseconds ( $10^{-24}$  s) to seconds and even much longer times.<sup>25,46–51</sup> This leads then also to the question of a theoretical understanding of these very different time scales for molecular primary processes by quantum chemical kinetics, and we shall address this question here with emphasis on the role of symmetries and the fundamental molecular processes of nuclear spin symmetry and parity violation (see also Refs. 3, 4). Fig. 1 provides a survey of this spectroscopic approach addressing also the role of symmetries, which we shall discuss in more detail in Section 2.

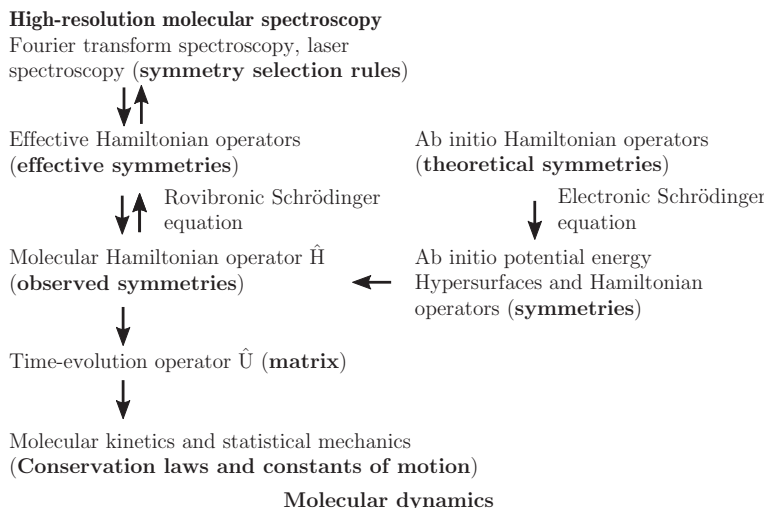
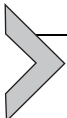


**Fig. 1** Scheme of the experimental approach to derive intramolecular dynamics (molecules in motion) from high-resolution spectroscopy. After Quack, M. *Molecules in Motion*. Chimia 2001, 55, 753–758.



## 2. Basic concepts of symmetry breakings, approximate constants of the motion and a survey of time scales for molecular processes

Motto: *Stationary states are the cemetery of quantum dynamics.*<sup>52</sup>

In the Schrödinger picture nonrelativistic (or semi-relativistic) quantum molecular dynamics is described by the time-dependent Schrödinger equation

$$i \frac{\hbar}{2\pi} \frac{\partial \Psi(\mathbf{q}, t)}{\partial t} = \hat{H}\Psi(\mathbf{q}, t) \quad (1)$$

where  $\mathbf{q}$  is implied to represent the collection of all spin and space coordinates of the molecule (or the single space coordinate for a simple one-dimensional model) and  $t$  is the time to be measured, say, by an atomic clock, with  $i = \sqrt{-1}$  and the generally time-dependent Hamiltonian  $\hat{H}$ . The solution of Eq. (1) can be written by means of the time evolution operator  $\hat{U}(t, t_0)$ , Eq. (2):

$$\Psi(\mathbf{q}, t) = \hat{U}(t, t_0)\Psi(\mathbf{q}, t_0) \quad (2)$$

satisfying an equivalent differential equation (Eq. 3).

$$i \frac{\hbar}{2\pi} \frac{\partial \hat{U}(t, t_0)}{\partial t} = \hat{H} \hat{U}(t, t_0) \quad (3)$$

For an isolated molecular system with a time-independent Hamiltonian ( $\hat{H}(t') = \hat{H}(t'')$  for all  $t'', t'$ ) one has

$$\hat{U}(t, t_0) = \exp \left[ -\frac{2\pi i}{\hbar} \hat{H} \cdot (t - t_0) \right] \quad (4)$$

and

$$\Psi(\mathbf{q}, t) = \sum_k c_k \varphi_k(\mathbf{q}) \exp [-2\pi i E_k t / \hbar] \quad (5)$$

where  $c_k$  are time-independent complex coefficients and the  $\varphi_k$  are the solutions of the time-independent Schrödinger equation

$$\hat{H} \varphi_k(\mathbf{q}) = E_k \varphi_k(\mathbf{q}) \quad (6)$$

with eigenvalues  $E_k$  and eigenfunctions  $\varphi_k(\mathbf{q})$ . The name stationary states arises from the fact that the “time-dependent states” for such a special case

$$\Psi_k(\mathbf{q}, t) = \varphi_k(\mathbf{q}) \exp [-2\pi i E_k t / \hbar] \quad (7)$$

result in a time-independent probability density  $P_k(\mathbf{q}, t) = P_k(\mathbf{q}, t')$  for all  $t, t'$ :

$$P_k(\mathbf{q}, t) = \Psi_k(\mathbf{q}, t)\Psi_k^*(\mathbf{q}, t) = |\Psi_k(\mathbf{q}, t)|^2 = |\varphi_k(\mathbf{q})|^2 \quad (8)$$

The time evolution operator  $\hat{U}(t, t_0)$  also solves the Heisenberg equation of motion for the operator  $\hat{Q}(t)$  related to some observable

$$\hat{Q}(t) = \hat{U}^\dagger(t, t_0)\hat{Q}(t_0)\hat{U}(t, t_0) \quad (9)$$

or also the Liouville–von Neumann equation for the statistical-mechanical density operator  $\hat{\rho}(t)$

$$\hat{\rho}(t) = \hat{U}(t, t_0)\hat{\rho}(t_0)\hat{U}^\dagger(t, t_0) \quad (10)$$

For further details and background we refer to Refs. 28, 29. These basic equations of time-dependent quantum dynamics describe the essence of quantum dynamical time-dependent molecular (and atomic) phenomena.

Now, instead of asking for some time-dependent phenomenon described, say, by the observable  $\hat{Q}_j(t)$ , one may ask the opposite question: What remains constant in some molecular process, when all these many  $\hat{Q}_j(t)$  change with time? The answer to this are the “constants of the motion”  $\hat{C}$ , which are the operators commuting with  $\hat{H}$  (see Refs. 2, 3, for instance)

$$\hat{H}\hat{C} = \hat{C}\hat{H} \quad (11)$$

These form a group, the group of the molecular Hamiltonian.<sup>3</sup> With the Heisenberg equation of motion (9) one can see in one line that they are, indeed, time independent

$$\hat{C}(t) = \hat{U}^\dagger(t, t_0)\hat{C}(t_0)\hat{U}(t, t_0) = \hat{U}^\dagger(t, t_0)\hat{U}(t, t_0)\hat{C}(t_0) = \hat{C}(t_0) \quad (12)$$

This follows from the unitary property of  $\hat{U}$

$$\hat{U}^\dagger\hat{U} = 1 \quad (13)$$

and because  $\hat{U}$  as a function of the Hamiltonian  $\hat{H}$  (Eq. 4) also commutes with  $\hat{C}$

$$\hat{U}\hat{C} = \hat{C}\hat{U} \quad (14)$$

With similar reasoning it follows from the equation for the density operator  $\hat{\rho}(t)$  that the expectation values of  $\hat{C}$  are time independent

$$\langle \hat{C}(t) \rangle = \text{tr}(\hat{\mathbf{Q}} \hat{C}) = \langle \hat{C}(t_0) \rangle \quad (15)$$

and also, if  $\Psi(\mathbf{q}, t)$  is an eigenfunction  $\zeta_n(t)$  of  $\hat{C}$  with eigenvalue  $C_n$ , one has

$$\langle \hat{C}(t) \rangle = \langle \zeta_n(t) | \hat{C}(t) | \zeta_n(t) \rangle = C_n \quad (16)$$

The  $C_n$  are “good quantum numbers,” which do not change with time. At first sight this might appear as a theoretical dead end, because, while showing that some observed properties, indeed, do not change at all with time, while others show slow and fast changes, it would not provide any further useful information on the dynamics on different time scales of molecular processes. Such information can, however, be obtained by considering various contributions of different magnitude in the molecular Hamiltonian:

$$\hat{H} = \hat{H}_0 + \hat{H}_1 + \hat{H}_2 + \hat{H}_3 \dots \quad (17)$$

Here  $\hat{H}_0$  will be assumed to be much larger than  $\hat{H}_1$ , which itself is much larger than  $\hat{H}_2$  and so forth. Such a description is in fact common in molecular spectroscopy where the different contributions correspond to different levels of accuracy and precision in the spectroscopic analysis. The procedure can, however, also be useful in a much more general way in the analysis of time-dependent molecular quantum dynamics.  $\hat{H}_0$  may be a zero order Hamiltonian contributing most of the energy and having a large symmetry group with correspondingly many constants of the motion  $\hat{C}_0$ .  $\hat{H}_1$  may contribute much less to the energy and have a smaller symmetry group with constants of the motion  $\hat{C}_1$ . Then some of the  $\hat{C}_0$  will not appear among the  $\hat{C}_1$  and thus, when considering the time-dependent dynamics of the molecular system described by  $(\hat{H}_0 + \hat{H}_1)$ , some of the observables  $\hat{C}_0$  will show a time dependence, and so forth also for the other contributions, which can be analyzed in a completely analogous fashion. The point in this procedure is, that when looking at the time variation of a  $\hat{C}_0$  it cannot arise, by symmetry, from the large  $\hat{H}_0$ , but must arise, say, from the possibly much smaller  $\hat{H}_1$ . Therefore, there would be no need to solve the time-dependent dynamics with  $\hat{H}_0$  at a precision corresponding to the small  $\hat{H}_1$ , because independent of any numerical errors arising in the use of  $\hat{H}_0$  we know exactly by symmetry that such errors or uncertainties cannot have an influence on the time variations of any of the  $\hat{C}_0$ , these changes must arise from  $\hat{H}_1$  (or other, further terms).

To use a common phrase, it allows one to weigh the captain directly, without having to weigh the captain with the ship and then the ship alone and get the captain's weight by obtaining the difference, which may have an uncertainty much larger than the weight of the captain.<sup>3</sup> For instance in the case of molecular parity violation the typical contributions of molecular energies at the level of  $\tilde{H}_0$  are in the range of 1 eV, say, while parity violating contributions are often in the sub-fēV range, say 100 aeV. Thus we can bridge a gap of 16 orders of magnitude by these symmetry considerations, an accuracy that is not achievable by electronic structure calculations on complex molecular systems.<sup>3,53–55</sup> The considerations work in the same way also for an experimental approach.<sup>47</sup> Fig. 2 shows a summary of the experimental scheme.<sup>47–52,56,57</sup>

We have used this approach as a very general procedure in analyzing the time scales for different intramolecular primary processes (Refs. 3, 46–52, 56 and references cited therein). Table 1 summarizes results from work of our group over many years for some selected primary processes. Of course, there is much work on various kinetic primary processes from other groups, which could be analyzed in a similar fashion, in principle.

One may say that, if certain processes occur by symmetry on a time scale which is well separated from other time scales, then they form “an island in the ocean of time.”<sup>52,88</sup> This view is represented graphically in Fig. 3.

Of the numerous results summarized in Table 1 we may consider here as one example the fast and mode-selective energy loss from a highly excited local C-H stretching excitation in organic molecules. It turns out that this energy flow is very different in alkylic ( $sp^3$ )R<sub>3</sub>C-H molecular structures,

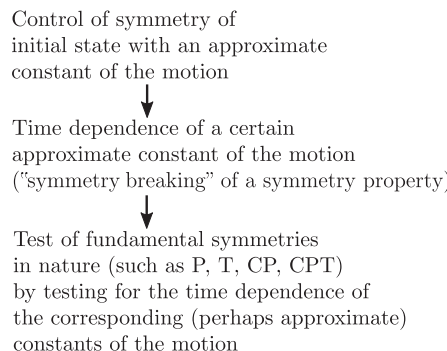


**Fig. 2** Scheme for control of symmetries and time evolution in molecular dynamics. Modified after Quack, M. *Comments on the Role of Symmetries in Intramolecular Quantum Dynamics*. *Faraday Disc.* 1995, 102, 90–93, 358–360.

**Table 1** Time scales for intramolecular primary processes as successive symmetry breakings.

Approximate constant of the motion	Symmetry breaking process (selected references)	Time scale
Quantum numbers of separate harmonic oscillators (for harmonic approximation in polyatomic molecules)	Selective vibrational stretch–bend Fermi resonance in $\text{R}_3\text{CH}$ <sup>48,49,58–64</sup>	10–200 fs
	Ordinary, weakly selective anharmonic couplings <sup>48,49,64–67</sup>	500 fs–10 ps
Quantum numbers of adiabatically separable anharmonic oscillators	“Vibrationally nonadiabatic” couplings $\text{R}-\text{C}\equiv\text{C}-\text{H}$ <sup>25,48–51,61,68–72</sup> $\Delta l$ coupling in $\text{C}_{3v}$ symmetric tops $\text{R}_3\text{CH}$ <sup>73</sup>	10 ps–1 ns
Structural identity for structures separated by high BO barriers	Tunneling processes <sup>44,45,74–77</sup>	1 ps to very long
Nuclear spin symmetry (separable nuclear spin–rotation–vibration states)	Violation of nuclear spin symmetry (rotation–vibration nuclear spin coupling) <sup>2,3,78</sup>	1 ns–1 s
Parity (space inversion symmetry)	Parity violation <sup>2,3,46,47,79–84</sup>	1 ms–1 ks (theory only)
Time reversal symmetry T	T-violation in chiral and achiral molecules? <sup>3,49–52,56,85–87</sup>	Molecular time scale not known (neither quantitative theory nor experiment) but known in SMPP
CPT Symmetry	Hypothetical CPT violation <sup>3,51,52,56,85</sup>	So far not found in any part of physics

Source: Modified after Quack, M. Fundamental Symmetries and Symmetry Violations From High Resolution Spectroscopy. In: *Handbook of High Resolution Spectroscopy*, Quack, M.; Merkt, F. (Eds.), Vol. 1, Wiley: Chichester, New York, 2011; pp. 659–722 (Chapter 18); Quack, M. Molecular Femtosecond Quantum Dynamics Between Less Than Yoctoseconds and More than Days: Experiment and Theory. In: *Femtosecond Chemistry*, Proc. Berlin Conf. Femtosecond Chemistry, Berlin (March 1993), Manz, J.; Wöste, L. (Eds.). Verlag Chemie: Weinheim, 1995; pp. 781–818 (Chapter 27); Quack, M. Molecules in Motion. *Chimia* 2001, 55, 753–758.

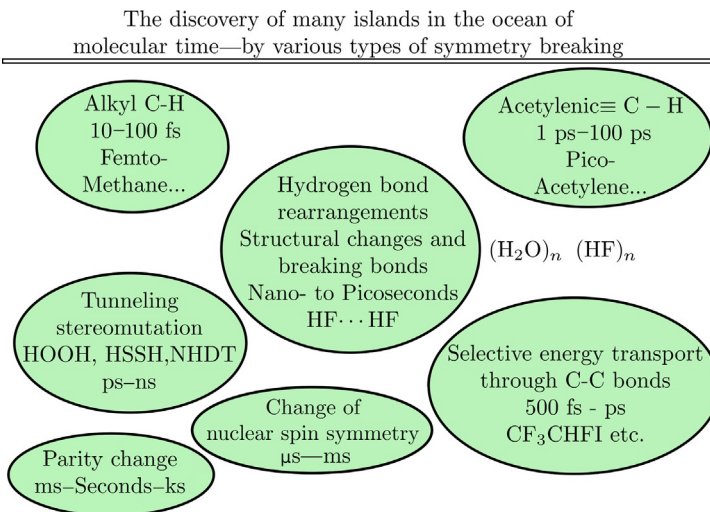


**Fig. 3** Islands in the ocean of time. Modified after Quack, M. *Naturwissenschaft als Beruf und Abenteuer: Servir sans Disparaître*. lecture ETH Zürich, 2014 (unpublished).

where it takes typically between 10 fs and 100 fs and in acetylenic ( $\text{sp}$ ) $\equiv\text{C}-\text{H}$  structures, where time scales a factor of 1000 longer between 10 ps and 100 ps can be found.<sup>25,48,49,58–68,88</sup> This has recently been reconfirmed in “bichromophoric” molecules with an alkylic CH infrared chromophore at one end of the molecule and an acetylenic infrared chromophore at the other end, ( $\text{H}-\text{C}\equiv\text{C}-\text{CH}_2\text{X}$ ).<sup>72</sup> Within the same molecule one can excite with a short pulse (100 fs) either one chromophore or the other, as they absorb in quite separate frequency ranges and indeed, the times for energy loss are orders of magnitude different even for the same molecule at similar (but not identical) energies.<sup>72</sup> An early example of a molecule with two different infrared chromophores ( $-\text{CH}_2\text{F}$  and  $-\text{CHDF}$ ) was investigated in the infrared multiphoton excitation and dissociation of a difluorobutane.<sup>89</sup>



Independent of whether the  $\text{CH}_2\text{F}$  or the  $\text{CHDF}$  chromophore was excited, a statistical distribution of products was found for time scales exceeding  $10^{-11}$  s, as accessible then. From this result, intramolecular energy relaxation to equilibrium could be inferred for times longer than 10 ps, which is an upper bound for the time for energy flow under these conditions. A lower bound can be

estimated for energy transfer over some distance using the speed of light as maximum speed. Thus for, say, 300 pm one finds 1 as ( $10^{-18}$  s) as a bound, which is a broad range indeed, but still instructive. Precise results can be obtained on specific systems by the approach summarized in Fig. 1 by numerous spectroscopic approaches,<sup>90</sup> where we mention in particular the chapters on infrared spectroscopy,<sup>66,91–93</sup> by either Fourier transform or laser techniques. Extensions to the microwave region at the low frequency end,<sup>94</sup> of particular importance for slower tunneling processes, and to visible and UV (also VUV) spectroscopy of relevance to electronic excitation<sup>95,96</sup> should be mentioned as well in an exemplary, not exhaustive, fashion.

Before addressing the approach to measure the effects from molecular parity violation at ultrahigh experimental resolution, appearing at the current long time frontier in Table 1, we shall discuss here two very simple theoretical limiting cases of solutions of the Schrödinger equation, Eq. (5), which illustrate the quantitative relation between certain energy contributions from the Hamiltonian and the various time scales. The first example concerns the evolution resulting from just two states in Eq. (5) with energies  $E_1$  and  $E_2$ , being rewritten in the form of Eq. (19)

$$\Psi(\mathbf{q}, t) = \frac{1}{\sqrt{2}} \exp(-2\pi i E_1 t / \hbar) [\varphi_1 + \varphi_2 \exp(-2\pi i \Delta E t / \hbar)] \quad (19)$$

with  $\Delta E = E_2 - E_1$ . The resulting measurable probability density is obtained from Eq. (8)

$$P(\mathbf{q}, t) = |\Psi(\mathbf{q}, t)|^2 = \frac{1}{2} |[\varphi_1 + \varphi_2 (-2\pi i \Delta E t / \hbar)]|^2 \quad (20)$$

This represents a periodic motion with a period

$$\tau = h / \Delta E \quad (21)$$

This type of periodic motion often describes simple tunneling motions well.<sup>38–40,44,45</sup> It also describes the spin dynamics in simple hyperfine interactions. It is used, indeed, also in atomic and molecular clocks, which are based on such a two state dynamics. For instance the current definition of the second in the SI (Système International) is based on the Cs atomic clock as an exact multiple of the period to the hyperfine interval  $\Delta E(\text{Cs})$  in the F = 3 to F = 4 hyperfine transition.

$$1 \text{ s} = 9192631770 \cdot \tau(\text{Cs}) \quad (22)$$

$$\Delta E(\text{Cs}) = (hc) \cdot 0.3066331899 \text{ cm}^{-1} \quad (23)$$

This hyperfine structure in the ground state of  $^{133}\text{Cs}$  arises from the interaction of the electronic spin  $s = 1/2$  of the unpaired valence electron and the nuclear spin  $I = 7/2$  for the  $^{133}\text{Cs}$  nucleus.<sup>97–99</sup> A simpler hyperfine structure arises in the H-atom MASER which is based on the  $F = 1$  to  $F = 0$  hyperfine transition in the  $^2\text{S}_{1/2}$  ground state of  $^1\text{H}$  where the electron spin ( $1/2$ ) interacts with the proton spin ( $1/2$ ). The ammonia MASER, on the other hand is based on a tunneling transition in  $^{14}\text{NH}_3$  and has been proposed as a molecular clock.<sup>100</sup>

The complex phase factor  $\exp(-2\pi i \Delta E t / \hbar) = \exp(-i\alpha)$  appearing in Eq. (20) for the atomic clock can be illustrated graphically in the Gaussian plane (see Fig. 4).

The unit vector in the Gaussian plane appears as the “hand of the atomic clock” which turns clockwise for positive times  $t$  completing one cycle in one period. In the time reversed state it turns anticlockwise ( $\exp(i\alpha)$ ).<sup>56,101</sup>

We might furthermore note here that together with the definition of the

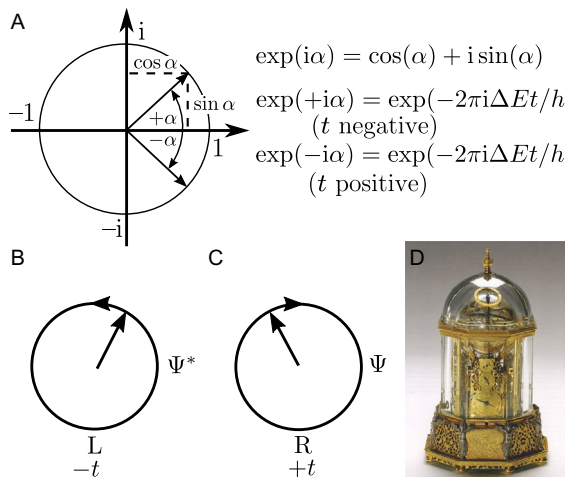


**Fig. 4** Illustration of the atomic clock: (A) The “hand of the atomic clock” represented by the vector of the complex phase factor in the Gaussian plane. (B) Time reversed state. (C) Time forward motion. (D) The “second clock” (Sekundenuhr) from Jost Bürgi showing the various “hands” (see also Ref. 102 and Kunsthistorisches Museum, Wien, with permission [www.khm.at/de/object/f9ae92df72](http://www.khm.at/de/object/f9ae92df72)). Modified after Quack, M. *Time and Time Reversal Symmetry in Quantum Chemical Kinetics*. In: *Fundamental World of Quantum Chemistry. A Tribute to the Memory of Per-Olov Löwdin*, Brändas, E. J.; Kryachko, E. S. (Eds.), Vol. 3. Kluwer Academic Publishers: Dordrecht, 2004; pp. 423–474; Quack, M. *Intramolekulare Dynamik: Irreversibilität, Zeitumkehrsymmetrie und eine absolute Moleküluhr*. *Nova Acta Leopoldina* 1999, 81 (Neue Folge (No. 314)), 137–173.

second the speed of light in vacuo (c) and the Planck constant  $h$  as appearing in Eqs. (21) and (23) are exactly defined constants in the new SI<sup>97,98</sup>

$$c = 299\ 792\ 458 \text{ ms}^{-1} \quad (24)$$

$$h = 6.626\ 070\ 15 \cdot 10^{-34} \text{ Js} \quad (25)$$

where Eq. (24) implies a definition of the meter (m) and Eq. (25) implies a definition of the kg (kilogram, through  $1 \text{ J} = 1 \text{ kg m}^2/\text{s}^2$ ). Thus in this sense the modern international system of units is entirely based on quantum dynamics and fundamental natural constants, removing the need for using artifacts as prototypes (as it was necessary for the “old” kg and the even older meter). We may conclude this general discussion with the picture of the historical first clock which was constructed to be able to measure time with an uncertainty of less than 1 s (Fig. 4D). Jost Bürgi built this clock between 1620 and 1627 and it includes explicitly a hand showing the seconds in addition to hands for the minute and the hour.<sup>102</sup> Jost Bürgi seems to have been the first to build a clock for an accurate measurement of the second which today is our time standard by use of an atomic clock. This clock was used in astronomy at the time and indeed the definition of the second until 1967 was based on an astronomical time, being defined then as an appropriate fraction of the tropical year 1900 ( $1a = 31556925.9747 \text{ s}$ ).<sup>97</sup> The name “second” derives from Latin “secunda” as a “second” division of the minute, minuta, into 60 parts, the minute (from Latin minutus, small, very small or “reduced into small pieces”) being the “first” division of the traditional time unit hour (hora) into sixty minutes, to provide here a complement in terms of historical etymology.

The second simple limiting case of Eqs. (1)–(5) to be discussed here is the exponential decay of an isolated state into a (quasi-)continuum<sup>41,42</sup> (see also Ref. 29). This corresponds to an exponential decay law for the probability of the initial state (the “survival probability”)

$$p(t) = \exp(-kt) = \exp(-t/\tau_d) \quad (26)$$

with

$$p(t) = |\langle \Psi(\mathbf{q}, t) | \Psi(\mathbf{q}, 0) \rangle|^2 = |\langle \Psi(\mathbf{q}, 0) | \Psi(\mathbf{q}, t) \rangle|^2 \quad (27)$$

and

$$\tau_d = 1/k = \frac{h}{2\pi\Gamma} \quad (28)$$

where  $\Gamma$  is the Full Width at Half Maximum (FWHM) of a probability distribution for the energy eigenstates

$$p(E) = \frac{1}{\pi} \frac{(\Gamma/2)}{(E - E_m)^2 + (\Gamma/2)^2} \quad (29)$$

Here  $E_m$  is the energy eigenvalue at the maximum of the Lorentzian (Cauchy) distribution given by Eq. (29). Eq. (28) has been derived originally using perturbation theory<sup>41</sup> as is also common in textbooks for what is often called “Fermi’s Golden rule,” but Bixon and Jortner<sup>42</sup> have derived it from an analytically exactly solvable model of multistate dynamics in a simple scheme with equidistant levels and constant couplings. We might note here that Eqs. (26)–(28) depend neither on perturbation theory nor on simple coupling models. Another simple exactly solvable model, which shows exponential decay of an initial state and provides explicit wavefunctions, is the harmonic oscillator. The time-dependent wavefunction for the exponential decay of a harmonic oscillator in an initial state given by a Lorentzian probability distribution over eigenstates according to Eq. (29) has been discussed in Refs. 103, 104. Of course, at long times the motion of the harmonic oscillator is periodic, the “recurrence time”  $\tau_r = 1/\nu$  being the period of the oscillator, which goes to infinity as the frequency and the energy interval  $\Delta E = h\nu$  go to zero. The recurrence times in statistically distributed spectra are much longer than for equidistant spectra, with the general inequality  $\tau_r \geq h\langle\varrho\rangle = h/\langle\Delta E\rangle$  with the average density of states  $\langle\varrho\rangle$ .<sup>105,106</sup> We might also note here the common procedure of introducing exponential decay by assigning complex values to energy eigenstates:

$$E_n = \text{Re}(E_n) - i \Gamma_n/2 \quad (30)$$

This convenient procedure removes the need for an explicit treatment of the large number of states in the (quasi-)continuum.<sup>107,108</sup> It introduces, however, non-Hermitian Hamiltonians and the need to handle effective Hamiltonian matrices which are complex symmetric.<sup>108–111</sup> We refer to Refs. 109–114 for a more detailed discussion of various further aspects.

We might finally note a very frequent misconception in particular in the textbook literature. The so-called “fourth uncertainty relation”

$$\Delta E \Delta t \geq \hbar/(4\pi) \quad (31)$$

following Heisenberg<sup>36,115</sup> is used as an equality in order to “derive” Eq. (28) (or also Eq. (21)) which then obviously needs some generous “adjustment of constants.” That this procedure is illegitimate should be

obvious and, indeed, the uncertainty product  $\Delta E \Delta t$  for the pair of exponential and Lorentzian functions is infinite, clearly consistent with the inequality, Eq. (31), but useless for “deriving” Eq. (28) (see Refs. 28, 29 for a critical discussion). We use the notion “Equation” (Eq.) in a generalized sense including strict equalities and also inequalities such as Eq. (31) as special cases.

While we do not intend to dig deeply into this matter, we note that the inconsistency of using the inequality (Eq. 31) as an equation to “derive” the lifetime  $\tau_d$  in Eqs. (26) and (28) from the width  $\Gamma$  in Eq. (29) does not depend on how one justifies Eq. (31) by fundamental theory. Even if one takes Eq. (31) as an empirically based inequality with  $\Delta E$  being the experimental root mean square deviation of an energy distribution and  $\Delta t$  the root mean square deviation of the lifetime distribution, then the “empirical” uncertainty product  $\Delta E \Delta t = \infty$  for the pair of Lorentzian and exponential distributions obviously satisfies the inequality in Eq. (31) perfectly, but cannot be used to derive a finite value of  $\tau_d$  from a finite  $\Gamma$ . On the other hand, the relation of Eq. (28) is an exact relation based on the Schrödinger equation (1).

Of course, the nontrivial nature of the theoretical foundations of Eq. (31) has been known for a long time, in fact from shortly after its original formulation<sup>115</sup> and the observation by Pauli<sup>116,117</sup> that time in quantum mechanics cannot be considered to be an “ordinary observable” with a definition of a self-adjoint time operator canonically conjugate to the Hamiltonian, which has an energy spectrum bounded from below. The theoretical foundations of Eq. (31) and the definition of time in quantum mechanics have found much interest and discussion in the literature, to which we refer with some selected references without any claim for completeness and with apologies to the many authors that may have been omitted<sup>116–125</sup> (see also Refs. 28, 29, 126, 127, 220).

The analysis of Lorentzian and also more complex structures of spectral line shapes and scattering resonances in terms of exponential (or possibly non-exponential) decay times has widespread use.<sup>29,51,70,71,112–114,127,163,217,218</sup> We conclude this general discussion with the example of the Z-Boson resonance discovered and analyzed at CERN in 1983. Fig. 5 shows the corresponding resonance line shape (analyzed with relativistic and further corrections) leading to what may be the shortest lifetime which has been quantitatively analyzed for a kinetic primary process.<sup>128,129</sup> The analysis with a model assuming three neutrino families for the decay products fits experiment giving a width  $\Gamma = 2.49$  GeV and a lifetime of only  $0.26$  ys ( $1$  ys =  $10^{-24}$  s). In this ultra short time light travels over a distance of less than  $0.1$  fm, a fraction only of the size of a nucleus. We shall see below that the Z-Boson as field particle of the parity violating weak nuclear force plays a special role also for the stereochemistry of chiral molecules.<sup>3,4,79–84,130,131,177</sup> In this context the first mentioning of the yoctosecond time scale in the chemical physics

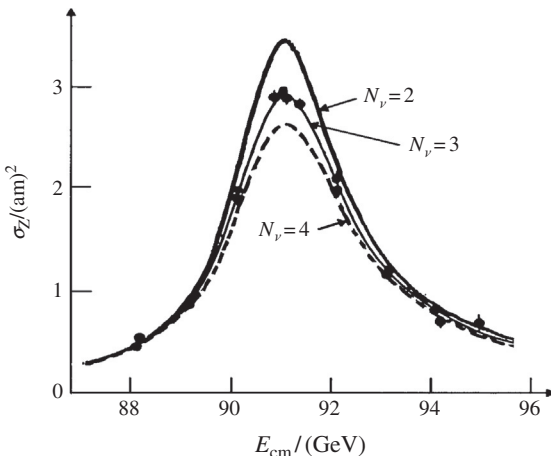


**Fig. 5** Lineshape of the resonance of the Z-Boson. The resonance cross section  $\sigma_z$  for producing the Z-Boson in collisions of positrons and electrons is shown as a function of the center of mass energy  $E_{\text{cm}}$ . The measured points are simulated with models assuming decay into 2, 3, or 4 neutrino families. Modified after Schopper, H.; Dilella, L. *60 years of CERN: Experiments and Discoveries*. World Scientific Publ.: Singapore, 2015; Schopper, H. *Lebenszeiten im Mikrokosmos von ultrakurzen bis zu unendlichen und oszillierenden*. In: *Nova Acta Leopoldina NF 81, Nr. 314*, Köhler, W. (Ed.). Wissenschaftliche Verlagsgesellschaft, Stuttgart, 1999; pp. 109–134.

literature seems to have been made at the First Femtosecond Chemistry Conference in Berlin 1993.<sup>25</sup> We might mention other short but slightly longer lifetimes of particles in the SMPP.<sup>221–223</sup> The top quark has a lifetime of 0.5 ys.<sup>224</sup> The lifetime of the Higgs Boson is not accurately known from experiment,<sup>222</sup> but a recent publication from the CMS collaboration provides bounds on the width  $\Gamma = 3.2 (+2.6/-2.2)$  MeV, corresponding to about  $\tau = 200$  ys<sup>225</sup> (see also Ref. 226). We note here the alternative interpretation of the “Higgs Boson resonance” at 125 GeV in a model, which gives, however, the same Z-Boson lifetime as the SMPP.<sup>227</sup>



### 3. Time dependence of exotic superpositions and the molecular quantum chameleon

#### 3.1 Elementary scheme for intramolecular coupling and symmetry breaking

We shall illustrate here the general summary of the previous section with a simple prototypical model for intramolecular couplings and primary processes by symmetry breaking. Fig. 6 shows an energy level scheme which is applicable to many types of intramolecular processes. Assume an  $\hat{H}_0$  which generates two sets of states of different symmetry which are uncoupled and

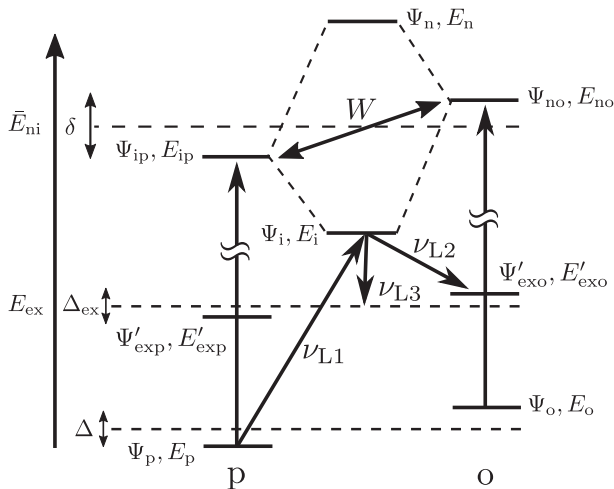


**Fig. 6** Elementary level scheme for intramolecular couplings (not to scale).

for which the symmetry labels (here p and o) are “constants of the motion.” A coupling Hamiltonian  $\hat{H}_1$  does not show this symmetry and leads to a coupling  $W$  breaking that symmetry generating a new set of eigenstates  $\Psi_i, E_i$  and  $\Psi_n, E_n$  from the zero order states  $\Psi_{ip}, E_{ip}$  and  $\Psi_{no}, E_{no}$ . As the Hamiltonian  $\hat{H}_1$  is assumed to be small, the coupling matrix element  $W$  is effective only for near resonant levels and most of the spectrum remains unaffected, i.e.  $\Psi_p, E_p$ ,  $\Psi_{exp}, E_{exp}$ ,  $\Psi_o, E_o$ , etc. retain their characteristic as eigenstates even if  $\hat{H}_1$  is included. The coupling is only important “near resonance,” i.e.  $W \simeq \delta = E_{no} - E_{ip}$ . Of course, this situation is well known in spectroscopy. The classic case is the anharmonic Fermi Resonance in  $\text{CO}_2$ .<sup>132</sup> The situation is well treated in many textbooks (see Ref. 66 for example, which we follow here, and Ref. 133 also for the early history). The situation is also applicable to other types of anharmonic resonances, such as Darling Dennison resonances, as well as rovibrational resonances, if treated as simple two-level perturbation problems. Table 1 contains many examples of this kind for more realistic systems including couplings of many levels, but the basics are the same. The couplings here lead to intramolecular rotational-vibrational redistribution usually on the fs to ps time scale, but extending also to ns.<sup>66,134</sup>

Another type of situation refers to nuclear spin-rotation–vibration coupling, which breaks the nuclear spin symmetry. Here  $\hat{H}_0$  would generate separate spectra for the nuclear spin isomers (say ortho and para, which can be connected to the labels o and p in Fig. 6) and we shall discuss the orders of magnitude of the much smaller couplings below. A further

example would be structural isomers, where  $\hat{H}_0$  describes the spectra of the separate isomers and  $\hat{H}_1$  allows coupling, say, by tunneling with a tunneling matrix element  $W$ . For all of these examples there exist, in fact, experimental results. A very interesting example of this kind are the enantiomers of chiral molecules where  $\hat{H}_0$  leads in the “high barrier limit” to a (nearly) degenerate set of states of the two structural isomers, which can be coupled by tunneling and for this situation experimental results exist as well.<sup>44,45</sup> There is, however, also a further coupling between the nearly degenerate chiral states, by means of the parity violating weak nuclear interaction.<sup>3,4,46,47</sup> So far this effect on the dynamics of chiral molecules has only been obtained by theory.<sup>3</sup> As has been shown in Ref. 47, the effect might be measured by using the scheme in Fig. 6 to generate “exotic superpositions” of the two enantiomers, which then are at the same time left handed and right handed structures of the chiral molecule thus “nonclassical” states generated from two different “classical” structures, like a “Schrödinger cat,” which is at the same time dead and alive (see Ref. 4). We have suggested, however, as a different animal analogy the “quantum chameleon,” which stays alive in the experiment in contrast to the Schrödinger cat, which dies with 50% probability in the experiment (Ref. 52, see discussion below). The simplest discussion of the scheme of Fig. 6 uses only the coupling of the two isolated levels  $E_{ip}$  and  $E_{no}$  in the scheme. We shall furthermore discuss the preparation of  $\Psi_{ip}$  by optical excitation of the coherent superposition of  $\Psi_i$  and  $\Psi_n$ . In a further scheme one can transform the isomer “p” into “o” by connecting  $E_p$  with a laser excitation to  $E_i$  (with  $\nu_{L1}$ ) followed by transfer to  $E_o$  or  $E_{exo}$  with a second laser pulse  $\nu_{L2}$ . Finally one can generate a coherent “nonclassical” superposition of  $\Psi_p$  and  $\Psi_o$  (or similarly of  $\Psi_{exp}$  and  $\Psi_{exo}$ ) by a sequence of laser pulses exciting  $E_i$  from  $E_p$  (with  $\nu_{L1}$ ) and then generate a superposition of both  $E_{exp}$  and  $E_{exo}$  starting from  $E_i$  (with  $\nu_{L3}$ ) shown by the various arrows. The particular properties of these last states are such that they allow for an ultrahigh resolution measurement of very small energy differences  $E_{exp}$  and  $E_{exo}$  or similarly also  $E_p$  and  $E_o$ . As pointed out in Ref. 47 and demonstrated in the proof of principle experiment of Ref. 83, one can by use of these quantum chameleon states make energy differences of the order of 100 aeV accessible to measurement as they are relevant for the parity violating energy differences  $\Delta_{pv}E$  between the ground states of enantiomers of chiral molecules (see also Refs. 3, 4). We shall thus in the following subsections address the following questions: (i) Can one prepare “exotic” superpositions of nuclear spin isomers? (ii) Can one prepare “exotic” nonclassical superpositions of structural isomers (such as syn- and anti- or cis- and trans-isomers)? (iii) Can one prepare superpositions of enantiomers generating thereby states of well-defined parity?

The short answer to these questions would, of course, be given by the quantum mechanical superposition principle:

If  $\Psi_A$  and  $\Psi_B$  are possible dynamical states, for instance also as solutions to Eq. (1), then

$$\Psi = a \Psi_A + b \Psi_B \quad (32)$$

is also a possible dynamical state. Thus the answer to the three questions above is by means of quantum mechanics: Yes.

While the answer might be obvious, there has been substantial debate on this question for some of these superpositions in the literature (see below) where occasionally their very existence was questioned, or they were excluded as “unphysical” or removed by a “superselection rule.” Indeed, the fact that such states  $\Psi$  exist, in principle, does not show, how they might be generated as “real” physical states in practice, and this was shown then by the scheme proposed in Ref. 47 for the particularly relevant question of parity violation. We shall illustrate here, how this idea can be used in a very general way for many processes and then discuss the current status for molecular parity violation. For definiteness we start out by providing the elementary analytical solutions for the two-level coupling following,<sup>66</sup> which can be consulted for more detail. Considering only the two zero order states  $\Psi_{ip}$  and  $\Psi_{no}$  one has an effective Hamiltonian matrix when including a coupling matrix element  $W = \langle \Psi_{ip} | \hat{H}_1 | \Psi_{no} \rangle$  which we assume for simplicity to be real, giving a real, symmetric matrix (in general, however, Hermitian)

$$H_{\text{eff}} = \begin{pmatrix} E_{ip} & W \\ W & E_{no} \end{pmatrix} \quad (33)$$

with

$$\delta = E_{no} - E_{ip} \quad (34)$$

One has two eigenvalues  $E_i$  and  $E_n$  summarized in the one Eq. (35) with alternatives + and –

$$E_{i,n} = \bar{E}_{n,i} \pm \frac{1}{2} \sqrt{4W^2 + \delta^2} \quad (35)$$

and a mean value of the energy,  $\bar{E}_{n,i}$

$$\bar{E}_{n,i} = \frac{E_{ip} + E_{no}}{2} = \frac{E_i + E_n}{2} \quad (36)$$

with eigenfunctions

$$\Psi_i = a \Psi_{ip} - b \Psi_{no} \quad (37)$$

$$\Psi_n = b \Psi_{ip} + a \Psi_{no} \quad (38)$$

and

$$a = \left( \frac{\sqrt{4W^2 + \delta^2} + \delta}{2\sqrt{4W^2 + \delta^2}} \right)^{1/2} \quad (39)$$

$$b = \left( \frac{\sqrt{4W^2 + \delta^2} - \delta}{2\sqrt{4W^2 + \delta^2}} \right)^{1/2} \quad (40)$$

One can furthermore give the explicit expression for the time evolution matrix.<sup>29,66</sup> For this we refer without loss of generality to an energy zero  $E_{ip} \stackrel{\text{def}}{=} 0$  and define an effective Hamiltonian in terms of parameters given as angular frequencies in Eq. (41):

$$\frac{2\pi H_{\text{eff}}}{\hbar} = \begin{pmatrix} 0 & V/2 \\ V/2 & D \end{pmatrix} \quad (41)$$

corresponding to introducing parameters  $D = 2\pi\delta/\hbar$  and  $V = 4\pi W/\hbar$  for convenience and furthermore an angular resonance frequency  $\omega_R$  with “resonance period  $\tau_R$ ”

$$\omega_R = \sqrt{V^2 + D^2} = 2\pi/\tau_R \quad (42)$$

The resonance period has the simple interpretation of being the period of motion of the superposition of the eigenstates  $\Psi_i$  and  $\Psi_n$  and in particular also when there is perfect resonance, i.e.  $E_{ip} = E_{no}$  and thus  $E_n - E_i = 2W$ . The time evolution matrix  $\mathbf{U}_{\text{eff}}$  for the two state system can be exactly derived by means of the eigenstates and eigenvalues of  $\mathbf{H}_{\text{eff}}$ <sup>29,66,135</sup>

$$\mathbf{Z}^{-1}(2\pi H_{\text{eff}}/\hbar)\mathbf{Z} = \Lambda = \text{Diag}(\lambda_1, \lambda_2) \quad (43)$$

$$\mathbf{U}_{\text{eff}}(t - t_0) = \mathbf{Z} \exp(-i\Lambda(t - t_0)) \mathbf{Z}^{-1} \quad (44)$$

with

$$\lambda_1 = \frac{1}{2} \left( D + \sqrt{V^2 + D^2} \right) \quad (45)$$

$$\lambda_2 = \frac{1}{2} \left( D - \sqrt{V^2 + D^2} \right) \quad (46)$$

$$x = \left[ \frac{1}{2} - \frac{D}{2\omega_R} \right]^{(1/2)} \quad (47)$$

$$\gamma = \left[ \frac{1}{2} + \frac{D}{2\omega_R} \right]^{(1/2)} \quad (48)$$

$$U_{11}(t) = \exp(-i\lambda_1 t) [x^2 + \gamma^2 \exp(i\omega_R t)] \quad (49)$$

$$U_{22}(t) = \exp(-i\lambda_1 t) [\gamma^2 + x^2 \exp(i\omega_R t)] \quad (50)$$

$$U_{12}(t) = U_{21}(t) = \exp(-i\lambda_1 t) xy [1 - \exp(i\omega_R t)] \quad (51)$$

where we have set  $t_0 = 0$  for simplicity of notation. We extend the simple two-level dynamics in the examples below to coherent radiative excitation of the multilevel scheme of Fig. 6. We solve the time-dependent Schrödinger equation for coherent radiative excitation treating the field as a z-polarized quasi-classical electromagnetic wave with electric field

$$E_z(\gamma, t) = |E_0(t)| \cos(\omega t + \eta' - k_\omega \gamma) \quad (52)$$

where  $E_0$  is related to the laser intensity by means of the simple practical equation

$$\left| \frac{E_0}{\text{Vcm}^{-1}} \right| \simeq 27.44924 \sqrt{\frac{I}{\text{Wcm}^{-2}}} \quad (53)$$

and the interaction energy with the field is treated in the electric dipole approximation, combining the phase factors into  $\eta$ , resulting for our case in

$$\hat{V}_{\text{el.dipole}} = -\hat{\mu}_z E_z(\gamma, t) \quad (54)$$

$$= -\mu_z |E_0(t)| \cos(\omega t - \eta) \quad (55)$$

and in a time-dependent Hamiltonian

$$\hat{H}(t) = \hat{H}_{\text{Mol}} - \mu_z |E_z(t)| \cos(\omega t - \eta) \quad (56)$$

where  $\hat{H}_{\text{Mol}}$  is the time-independent Hamiltonian of the isolated molecule. This results in a time-dependent matrix Schrödinger equation for time-dependent coefficients  $b_k$  of the multilevel system

$$i \frac{\hbar}{2\pi} \frac{d\mathbf{b}}{dt} = \mathbf{H}(t) \mathbf{b}(t) \quad (57)$$

We have solved this equation for the simple examples below numerically in the quasi-resonant approximation,<sup>135–137</sup> which is an excellent approximation for our conditions. We also note that excitation in the magnetic dipole approximation would follow equivalently with a simple change of parameters (see Ref. 137, where one can also find computer program packages). We shall give now some exemplary solutions, providing in general the time-dependent populations  $p_k = |b_k|^2$ . We may furthermore

note here that the quasiresonant approximation for the radiative excitation with two levels results in an effectively time-independent Hamiltonian similar to Eq. (41) with  $V$  being replaced by an electric dipole coupling matrix element, which can be computed with the practical Eq. (58)<sup>29,135,137</sup>:

$$|V_{kj}/\text{s}^{-1}| = 8.682273 \times 10^7 |M_{kj}/\text{D}| \sqrt{I/(\text{W cm}^{-2})} \quad (58)$$

with the matrix element  $M_{kj}$  being inserted in Debye units (D) and the pre-factor rounded to 7 significant digits. To within some further approximations the numerical results presented below can also be obtained as sequential processes involving analytical calculations using two-level formulae.<sup>158</sup>

### 3.2 Violation of nuclear spin symmetry and the superposition of nuclear spin isomers

We use the scheme in Fig. 6 as a prototypical, simplified example for coupling in nuclear spin isomers. The parameters are chosen such, that they correspond to typical hyperfine couplings, where  $W/h$  is on the order of MHz if quadrupole nuclei with nuclear spin ( $I \geq 1$ ) are involved. The coupling is much smaller, say, kHz range for molecules including only nuclei with spin (1/2), but relatively large values have been found for radicals.<sup>144</sup> Because of the difficulty of satisfying the near resonance condition  $|W| \approx |E_{\text{ip}} - E_{\text{no}}|$  in sparse spectra, when couplings are so small only relatively few examples with an explicit high-resolution spectroscopic analysis for such couplings between ortho and para nuclear spin isomers (also meta, etc.) have been reported in the literature<sup>138–144</sup> (see also the references in Ref. 3). There is no doubt, however, that at high density of states relevant in polyatomic molecules at high rovibrational excitations (also electronic) such couplings are important and abundant. There do not seem to exist any direct observations of the time-dependent primary process of intramolecular change of nuclear spin symmetry in isolated molecules, although such experiments have been proposed for quite some time.<sup>57</sup> In many experiments on polyatomic molecules in supersonic jet expansions nuclear spin symmetry conservation on short time scales has been found (Refs. 145–153 and references cited therein). For the diatomic molecule H<sub>2</sub> ortho and para nuclear spin isomers have been known to be stable in bulk even for months.<sup>154,155</sup> On the other hand slow conversion of nuclear spin isomers has been observed both in the bulk gas and condensed phases (Refs. 78, 154, 155 and further references cited there and in Refs. 45, 153). The question of the existence of superpositions of nuclear spin isomers has led to some debate in the past, as there is a “folk myth” among spectroscopists that such superpositions cannot be prepared. Such a statement can even be found in the recent literature, where such superpositions were identified

as “unphysical.”<sup>156</sup> We have pointed out repeatedly in the past in such discussions, however, that one can prepare these superpositions for instance with the scheme of Ref. 47 (see Refs. 57, 157, 158, for example). Here we use the basic scheme of Fig. 6, with parameters adjusted to a typical situation of nuclear spin symmetry coupling in infrared spectra of polyatomic molecules to demonstrate the three main processes connected to this scheme:

- (i) Preparation of an excited state  $E_{ip}$  and oscillatory probability transfer to  $E_{no}$ .
- (ii) Nuclear spin isomerization from a para to an ortho isomer state with the two-pulse sequence  $\nu_{L1}$  followed by  $\nu_{L2}$
- (iii) Generation of a superposition of nuclear spin isomers with the sequence of pulses  $\nu_{L1}$  and  $\nu_{L3}$ .

The numerical parameters of the model are given in Table 2. They correspond in magnitude to, say, rovibrational intervals in an asymmetric rotor like H<sub>2</sub>O,<sup>149,150</sup> but with stronger couplings more typical of quadrupole nuclei such as ClSSCl which has found interest in this context as also in parity violation<sup>77,140</sup>. We have, however, not retained the complexity of the multilevel structure arising from the many magnetic sublevels. The basic features and orders of magnitude, however, are retained in the simple model. For definiteness we also give here the structure of the wavefunctions for the simple case of ortho- and para- isomers in a proton spin  $s = 1/2$  case such as in <sup>1</sup>H<sub>2</sub><sup>16</sup>O.<sup>149,150</sup> We denote the single nuclear spin functions  $\alpha$  (for  $m_s = +1/2$ ) and  $\beta$  (for  $m_s = -1/2$ ) and indicate in

**Table 2** State energies for Fig. 6 and transition moments.<sup>a</sup>

State	$E_{state}/(hc \text{ cm}^{-1})$	Transition moments
p	0	$\langle \Psi_p   \mu   \Psi_{ip} \rangle = 1.05 \text{ D}$
o	0.1	$\langle \Psi_o   \mu   \Psi_{no} \rangle = 0.95 \text{ D}$
exp	5	$\langle \Psi_{exp}   \mu   \Psi_{ip} \rangle = 1.05 \text{ D}$
exo	5.02	$\langle \Psi_{exo}   \mu   \Psi_{no} \rangle = 0.95 \text{ D}$
ip	$\bar{E}_{in} - \delta/2$	
no	$\bar{E}_{in} + \delta/2$	
i	$\bar{E}_{in} - \frac{1}{2} \cdot \sqrt{4 \cdot W^2 + \delta^2}$	
n	$\bar{E}_{in} + \frac{1}{2} \cdot \sqrt{4 \cdot W^2 + \delta^2}$	

<sup>a</sup> $\bar{E}_{in}/(hc)$  can be assumed to be  $3300 \text{ cm}^{-1}$  corresponding to an infrared transition, but in the quasi-resonant approximation it could also take other values without change in the results.

parentheses the numbering of the nucleus considered (say proton 1 and proton 2 with  $\alpha(1)$  and  $\alpha(2)$ , etc.). The nuclear spins  $I_{1,2}$  combine accordingly to a total spin  $I$  ( $I_1 = I_2 = s = 1/2$  for the example)

$$|I_1 - I_2| \leq I \leq I_1 + I_2 \quad (59)$$

with integer steps in the quantum number  $I$ , thus with two protons we have  $I = 0$  or  $1$ . We obtain three normalized symmetrical nuclear spin functions with  $I = 1$  and  $M_I = 0, \pm 1$

$$\varphi_{s1} = \frac{1}{\sqrt{2}} [\alpha(1)\beta(2) + \alpha(2)\beta(1)] \quad \text{with } M_I = 0 \quad (60)$$

$$\varphi_{s2} = \alpha(1)\alpha(2) \quad \text{with } M_I = 1 \quad (61)$$

$$\varphi_{s3} = \beta(1)\beta(2) \quad \text{with } M_I = -1 \quad (62)$$

There is one antisymmetrical function with  $I = 0$  and  $M_I = 0$

$$\varphi_a = \frac{1}{\sqrt{2}} [\alpha(1)\beta(2) - \alpha(2)\beta(1)] \quad (63)$$

The total wavefunction can be written approximately as a product of the combined electronic (spin and space) and vibration rotation function  $\Psi_{evr}$  and the nuclear spin function, where we assume that the electronic part is already properly antisymmetrized. If we assume nuclear spin symmetry conservation one would have:

$$\Psi_{tot,j} \simeq \Psi_{evr,j} \cdot \varphi_{spin,j} \quad (64)$$

but the exact total wavefunction including coupling between states of different nuclear spin symmetry will be:

$$\Psi_{tot \text{ exact}} = \sum_j c_j \Psi_{tot,j} \quad (65)$$

Often there will be a leading term in the sum with one  $|c_k| \simeq 1$ , but if there is mixing as for the upper levels in Fig. 6 there may be two  $c_j$  of similar absolute magnitude and in the limit of very high density of states with many states mixing one may have to retain many terms in the sum. However, all individual terms as also the total wavefunction must satisfy the generalized Pauli principle for the two Fermion nuclei concerning the symmetry with respect to the permutation (12) of the two nuclei

$$(12)\Psi_{tot} = -\Psi_{tot} \quad (66)$$

Eq. (66) is a special case of the generalized Pauli principle for  $N$  different kinds of particles ( $n_i$  each kind) and the direct product of symmetric groups  $S_{n_i}$  for these

$$S_{n_1, n_2, n_3, \dots} = \prod_{i=1}^N S_{n_i} \quad (67)$$

where the character under the group operation  $Q$  is given by Eq. (68):

$$\chi_Q = \prod_{i=1}^{N_F} (-1)^{P_{iQ}} \quad (68)$$

$P_{iQ}$  is the parity of the permutation of the  $i$ th kind of Fermions (total number  $N_F$ ) in the group element  $Q$ . If  $Q$  permutes only bosons we have  $\chi_Q = +1$  (see Refs. 2, 3).

Fig. 6 represents the typical situation where most states are well described by Eq. (64). Then one can identify two separate sets of states, one with a symmetric nuclear spin function (with  $I = 1$ , called the ortho nuclear spin isomer) and one with  $I = 0$  (called the para isomer). We may note in passing that neither for  $H_2$  nor for  $H_2O$  so far any pairs of strongly mixing ortho and para states have been identified by high-resolution spectroscopy, although they certainly must exist at high excitation. This situation leads also to the consequence, that in general the relative energies of the nuclear spin isomers are not as precisely known as the relative energies within each isomer. This is similar to other types of isomers, where the isomerization energy has to be determined in addition to the very accurate level positions within each isomer. For instance, the isomerization energy between the ortho and para isomers of  $H_2$  has only recently been determined accurately by a special experimental technique<sup>159</sup> although it had been calculated accurately by theory for some time and was, of course, known at lower accuracy also by experiment. In the few molecules where mixing levels have been measured by high-resolution spectroscopy, one has, of course, direct access to the isomerization energy as in the scheme of Fig. 6. We shall now discuss in an exemplary way different kinetic processes for such a scheme. If we consider as the simplest example only the two coupled levels  $E_{ip}$  and  $E_{io}$  of the para and ortho isomers at perfect resonance  $E_{ip} = E_{io}$  and  $W/h = 1$  MHz then with the energy splitting of eigenstates ( $2W$ ) one has a periodic oscillation between the ortho and para states with period  $\tau = h/(2W) \simeq 0.5$   $\mu$ s. If the resonance is not exact the time evolution follows from Eqs. (45)–(51). The question arises, how to prepare the initial state

and for this we consider radiative excitation in a scheme with initial population in the ground state, which is  $p$  with energy  $E_p$  in Fig. 6. Given the selection rules,  $\Psi_{ip}$  acts as “chromophore state” (see Table 2), but we carry out the calculation in the basis of spectroscopic eigenstates with ( $E_p$ ,  $E_i$ , and  $E_n$ ) as relevant states in the solution of Eq. (57) and numerical parameters as given in the caption of Fig. 7.

One can nicely see the build-up of population in a coherent superposition ( $\Psi_i$ ,  $\Psi_n$ ) starting from  $\Psi_p$  at time zero and projecting the time-dependent wavefunction after the pulse onto the ortho and para zero order states one sees the starting population in  $\Psi_{ip}$  followed by an oscillation toward  $\Psi_{no}$  and back with a period of 500 ns as expected, describing thus perfectly well a realistic situation for such a spectroscopic experiment with ortho–para conversion in an isolated molecule.

As a next example we consider excitation of a para state  $p$  with a laser frequency  $\nu_{L1}$  to the eigenstate with  $E_i$  and then generating an excited ortho state at  $E_{exo}$  (Fig. 8) using a laser frequency  $\nu_{L2}$ .

Finally, we consider the preparation of the superposition of a pair of ortho and para states (Fig. 9) using a long laser pulse of frequency  $\nu_{L1}$  to prepare  $\Psi_i$  followed by a short laser pulse at 1.3  $\mu$ s to generate the superposition of  $\Psi_{exo}$  and  $\Psi_{exp}$ .

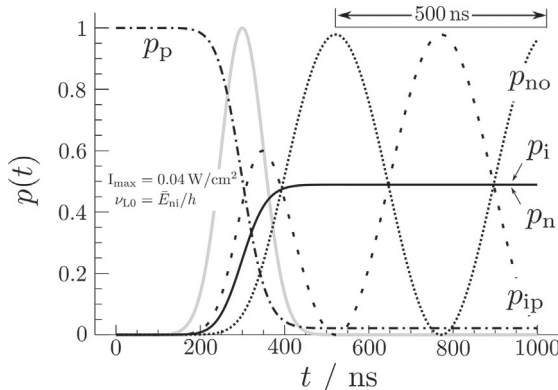


**Fig. 7** For the scheme in Fig. 6 with  $\delta = 0$  and  $W/h = 1$  MHz, i.e.,  $E_n - E_i = h \cdot 2$  MHz, we have the time evolution starting from 100% population in the ground state  $p$  ( $p_p = 1$ ) excited with a laser (peak intensity of  $0.04$  W/cm $^2$ , Gaussian time profile with  $\Delta t_{FWHM} = 2\sqrt{2\ln 2} \cdot 50$  ns = 117.7 ns and frequency  $\nu_{L0} = \bar{E}_{ni}/h = 0.5 \cdot (E_i + E_n)/h$ ). The gray line shows the normalized laser intensity. For this particular condition  $\Psi_i$  and  $\Psi_n$  are equally populated ( $p_i = p_n$ ). The dashed and dotted oscillating lines show the projection onto the unperturbed states  $\Psi_{ip}$  and  $\Psi_{no}$  with the expected oscillation period of 500 ns for the probabilities  $p_{ip}$  and  $p_{no}$ .

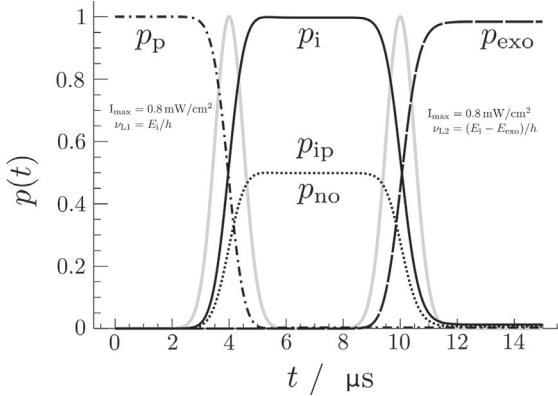


**Fig. 8** For the scheme in Fig. 6 with  $\delta = 0$  and  $W/h = 1$  MHz, i.e.,  $E_n - E_i = h \cdot 2$  MHz, we have the time evolution starting from 100% population in the ground state  $p$  ( $p_p = 1$ ) excited to  $\Psi_i$  with a laser (peak intensity of  $0.8$  mW/cm $^2$ , Gaussian time profile with  $\Delta t_{\text{FWHM}} = 2\sqrt{2 \ln 2} \cdot 0.5$   $\mu$ s =  $1.177$   $\mu$ s and frequency  $\nu_{L1} = E_i/h$ ) and with a second laser pulse with the same intensity and length but with frequency  $\nu_{L2} = (E_i - E_{\text{exo}})/h$  to the excited ortho state  $\Psi_{\text{exo}}$ . The gray line shows the normalized laser intensity of the first and the second laser pulse, each normalized independently to 1. The dotted line shows the projection onto the unperturbed states  $\Psi_{\text{ip}}$  and  $\Psi_{\text{no}}$ .

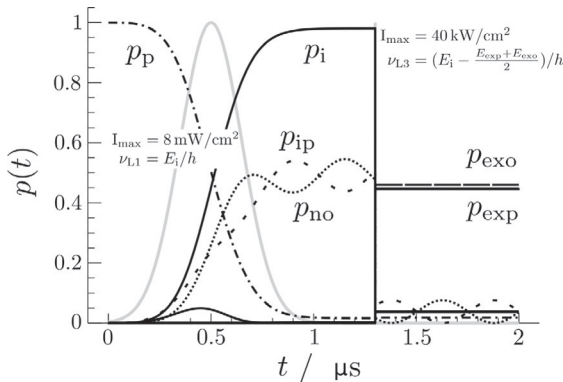


**Fig. 9** For the scheme in Fig. 6 with  $\delta = 0$  and  $W/h = 1$  MHz, i.e.,  $E_n - E_i = h \cdot 2$  MHz, we have the time evolution starting from 100% population in the ground state  $p$  ( $p_p = 1$ ) excited to  $\Psi_i$  with a laser (peak intensity of  $8$  mW/cm $^2$ , Gaussian time profile with  $\Delta t_{\text{FWHM}} = 2\sqrt{2 \ln 2} \cdot 0.15$   $\mu$ s =  $0.3532$   $\mu$ s and frequency  $\nu_{L1} = E_i/h$ ) and with a second shorter and stronger laser pulse (peak intensity  $40$  kW/cm $^2$ , Gaussian time profile with  $\Delta t_{\text{FWHM}} = 2\sqrt{2 \ln 2} \cdot 0.05$  ns =  $0.1177$  ns and frequency  $\nu_{L3} = (E_i - (E_{\text{exp}} + E_{\text{exo}})/2)/h$ ) to the two excited ortho and para states  $\Psi_{\text{exo}}$  and  $\Psi_{\text{exp}}$ . The gray line shows the normalized laser intensity of the first and the second laser pulse, each normalized independently to 1. The width of the second pulse at  $1.3$   $\mu$ s is not visible on this scale giving the sharp vertical line. The dotted line shows the projection onto the unperturbed states  $\Psi_{\text{ip}}$  and  $\Psi_{\text{no}}$ .

Obviously this time-dependent state is perfectly “physical,” it can be prepared and will then show after the pulse an oscillation with a period given by  $\tau = h/\Delta E_{\text{op}}$  where  $\Delta E_{\text{op}} = E_{\text{o}} - E_{\text{p}}$  if one returns to a ground state pair or it could be given by  $\Delta E_{\text{exop}} = E_{\text{exo}} - E_{\text{exp}}$  for an excited pair as in Fig. 9. The oscillation could be detected by time resolved spectroscopy (see also the corresponding discussion in Section 3.3). An accurate measurement of the oscillation periods would provide an accurate value for the energy differences ( $E_{\text{exo}} - E_{\text{exp}}$  or  $E_{\text{o}} - E_{\text{p}}$ ), which in this case would also be available from the relevant high-resolution spectroscopic combination differences.

We shall not discuss in detail the many further results that we have considered for various sets of parameters. For the case of nuclear spin symmetry mixing, typically one should consider situations with large values of  $\delta$ , as a close “accidental” resonance is unlikely. However, also for large  $\delta$  rather similar results can be obtained with appropriate changes. Rather than relying on an accidental resonance one can induce a close degeneracy by applying external fields, as has been elegantly done in the pioneering experiments of Ozier and coworkers in 1970/71 for methane ( $^{12}\text{CH}_4$ )<sup>138,160</sup> (see also Refs. 161, 162). In methane one has three nuclear spin isomers which we can label by their “motional” symmetry A( $I = 2$ , “meta”), E( $I = 0$ , “para”) and F( $I = 1$ , “ortho”) (with the total Pauli allowed nuclear spin in parentheses, but one also frequently uses ortho, meta, and para with relative abundances 9/16, 5/16, 2/16 (Refs. 145–148), ortho being the most and para the least abundant at high temperature by convention). It turns out that at rotational angular momentum quantum number  $J = 2$  methane has a triplet of levels, a pair of closely degenerate E levels of different parity ( $E^+$  and  $E^-$ ) and an  $F_1^-$  level 0.000266 cm<sup>-1</sup> higher. At a magnetic field of about  $B = 0.2$  Tesla the  $F_1^-$  ( $M_F=0$ ,  $I=1$ ,  $M_I=+1$ ) level becomes degenerate with the  $E^-$  ( $I=0$ ,  $M_F=M_I=0$ ) level, thus resulting in a perfect mixing of the two nuclear spin isomers. From the splitting at the avoided crossing one can derive the coupling  $W$  and one would have a level scheme such as in Fig. 6 with  $\delta = 0$ , disregarding the other levels. Ozier et al. did not consider the further effect of parity violation, which was discussed by us later as well.<sup>3,46,162</sup> In principle this would lead to a further avoided crossing between two levels of different parity shown in the lower part on the right-hand side of Fig. 10. If this were measurable by high-resolution spectroscopy, one could measure the effect of parity violation in methane from this avoided crossing. Our preliminary calculations on parity violating potentials in methane<sup>79</sup> indicate, however, that the effect would be too small to be accessible with current experimental technology. Thus for detecting parity violation in molecules another approach would be more promising

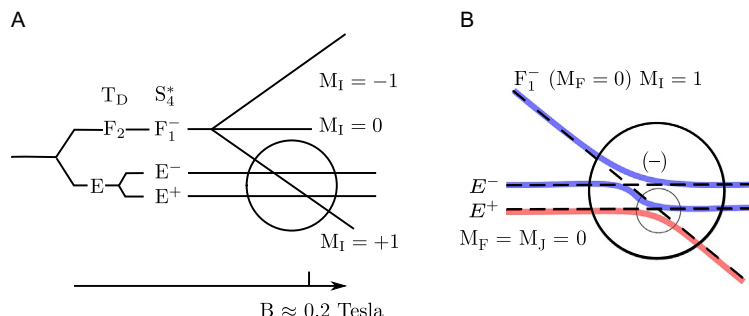


**Fig. 10** Scheme for crossings and avoided crossings in sublevels of the same rotational angular momentum quantum number  $J = 2$  in methane  $\text{CH}_4$  but different symmetry and nuclear spin ( $I = 0$  with  $E$  and  $I = 1$  with  $F$ ) in the experiment by Refs. 138, 160. (A) This shows the overall level behavior as a function of magnetic induction  $B$ . The crossing is supposed to occur at  $0.2\text{ T}$ <sup>161,162</sup>, and each line would have a further smaller Zeeman splitting into five levels with  $M_J = 2, 1, 0, -1, -2$ . Furthermore, the crossings in the *circle* are avoided, as shown in detail in (B). Here, only the sublevels with the same total angular momentum  $F$  ( $= 2$  for the example with  $J = 2$ ) are shown with  $M_F = 0$  (there are similar schemes for the other values of  $M_F$ ). The crossing in the *large circle* between the  $F_1^-$  and  $E^-$  levels is strongly avoided, whereas the crossing between levels of positive and negative parity in the *small circle* could at most be weakly avoided by the parity violating weak nuclear force. We assume that the zero order (*dashed lines*)  $E^+$  level is below  $E^-$  similar to Ref. 161, where parity violation was not considered, but the opposite ordering is also possible and would result in otherwise equivalent schemes. The parity violation at the crossing would mix levels of different parity, creating possibly chirality<sup>162</sup>. It could be observed either by directly mapping the magnetic dipole transition frequencies at extremely high resolution<sup>160</sup> or by observing magnetic dipole forbidden transitions but the effects are expected to be very small<sup>79</sup> (see also Ref. 3). Modified after Pepper, M. J. M.; Shavitt, I.; von Ragué Schleyer, P.; Glukhovtsev, M. N.; Janoschek, R.; Quack, M. Is the Stereomutation of Methane Possible? *J. Comp. Chem.* 1995, 16 (2), 207–225.

(see below). For a more detailed discussion of the mixing effects in methane we refer to Refs. 3, 46, 162. We may mention here that level crossings have more generally a number of interesting consequences in a variety of situations in spectroscopy and electronic structure theory.<sup>3,28,29,95,163–165</sup>

### 3.3 Mixing and superposition of structural isomers: The molecular quantum switch

Another interesting example for the application of the scheme of Fig. 6 is the molecular quantum switch recently demonstrated for the case of meta-D-phenol.<sup>166–168</sup> Phenol  $\text{C}_6\text{H}_5\text{-OH}$  in its electronic ground state has a planar  $C_s$  geometry with two equivalent potential minima in its Born-Oppenheimer potential, because of the nonlinear bent C-O-H structure. The potential barrier to internal rotation (torsion) of the C-OH group

is modest ( $\approx 1000 \text{ cm}^{-1}$ ) and there is a ground state tunneling splitting in the MHz range,<sup>166–168</sup> with correspondingly delocalized wavefunctions. When substituting in either ortho or meta position with a D-atom one breaks the symmetry in the effective tunneling potential because of zero point energy effects which are much larger than the phenol tunneling splitting.<sup>167</sup> This then leads to localized wavefunctions in the syn- and anti-geometry of the OH group with respect to D (see Fig. 11). At low energies one has thus two sets of geometrical isomers (anti- and syn- instead of p and o in Fig. 6). The ground state energy difference was determined accurately by a careful high-resolution spectroscopic analysis as  $\Delta E = (hc) \cdot 0.82 \text{ cm}^{-1}$ .<sup>166</sup> Thus structural identity is a “constant of the motion” at low energy. At high torsional excitation the localized states are coupled by tunneling leading to delocalized eigenstate pairs such as  $\Psi_i, E_i$  and  $\Psi_n, E_n$  in the scheme of Fig. 6. In contrast to the nuclear spin isomers, where such an analysis does not yet exist, we have been able to carry out the complete high-resolution analysis and quantum dynamical simulation for this “real” molecular system of m-D-phenol.<sup>166–168</sup>

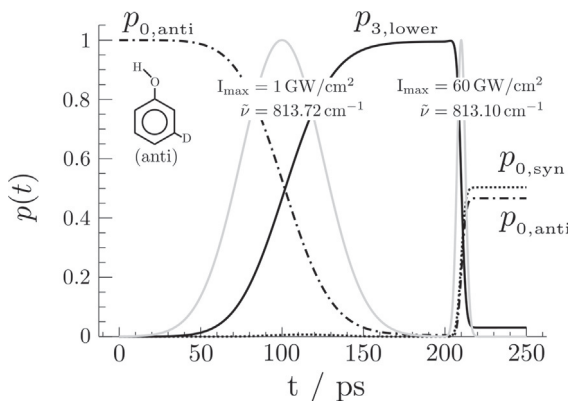


**Fig. 11** Time evolution for the two-pulse excitation scheme from 0(anti) to 3(lower) and from 3(lower) to 0(anti) and 0(syn) with the notation  $\nu(\text{isomer})$ . The parameters of the two laser pulses are  $\Delta t_{\text{FWHM}} = 2\sqrt{2 \ln 2} \cdot 25 \text{ ps} = 58.87 \text{ ps}$ , peak intensity  $1 \text{ GW/cm}^2$  and with a wavenumber of  $\tilde{\nu} = 813.72 \text{ cm}^{-1}$  (first pulse, resonant with 0(anti) to 3(lower) transition, and second pulse with  $\Delta t_{\text{FWHM}} = 2\sqrt{2 \ln 2} \cdot 2.5 \text{ ps} = 5.887 \text{ ps}$  and peak intensity  $60 \text{ GW/cm}^2$  and with a wavenumber of  $\tilde{\nu} = 813.10 \text{ cm}^{-1}$  (3(lower) to 0(anti) and 0(syn)). The gray line shows the normalized laser intensity of the first and the second laser pulse, each normalized independently to 1 (cf Fig. 13 from Ref. 168 where one finds also the parameters used for the simulation in the model, as simplified here). Equivalent results are obtained when starting from the syn-isomer or also from a racemate, with the appropriate changes taking the mixture of syn and anti.

In molecular quantum systems with localized eigenstates of well-defined quasi-classical molecular structures at low energies showing a transition to delocalized eigenstates by tunneling at high energies one observes a phenomenon, which we call “tunneling switching”<sup>169</sup> allowing for a variety of interesting quantum dynamical experiments. They can be designed either for use as quasi-classical molecular switches, but also for use as molecular quantum switches offering completely new possibilities. Meta-D-phenol has been analyzed by full-dimensional wavepacket simulations in this context<sup>168</sup> based on the high-resolution spectroscopic experiments and including all 33 vibrational degrees of freedom in the quasiadiabatic channel reaction path Hamiltonian approximation.<sup>74,75</sup> Here we reproduce the most significant result for the use as a molecular quantum switch on the basis of the simple scheme of Fig. 6. Fig. 11 shows the simulation of the quantum switch in terms of the relevant populations (anti = p in Fig. 6, syn = o,  $\Psi_i$  corresponds to  $\Psi_{3\text{lower}}$ , which is the lower tunneling level with 3 quanta of the torsion with large tunneling splitting of about  $16 \text{ cm}^{-1}$ ). With a sequence of two laser pulses shown in Fig. 11 one generates at  $t > 220 \text{ ps}$  a superposition of the syn- and anti-structures  $\Psi(t) = a \Psi_{0\text{syn}} + b \Psi_{0\text{anti}}$  in the torsional ground state. After the end of the pulse sequence the nearly equal probabilities  $|a|^2$  and  $|b|^2$  and also the 33-dimensional probability density in structural space do not change with time. However, because of the complex phase factors there is a periodic change of the spectra as analyzed in<sup>168</sup>. The period corresponds to the ground state energy difference of the two isomers ( $hc \cdot 0.82 \text{ cm}^{-1}$ )

$$\tau = \frac{\hbar}{E_{0\text{syn}} - E_{0\text{anti}}} \approx 40 \text{ ps} \quad (69)$$

The change of the spectra is like the “change of color of a quantum chameleon.” It is quite pronounced and can be understood by the periodic change with time of the approximate symmetry of the superposition state between symmetric and antisymmetric with respect to the plane containing the C-O bond and perpendicular to the phenyl ring, while the eigenstates of the well separated tunneling sublevels at high torsional excitation are also approximately symmetrical and antisymmetrical.<sup>168</sup> The result in Fig. 11 is analogous to the result in Fig. 9, now with times and other properties being obtained from the high-resolution spectroscopy of the real molecule m-D-phenol. The simple scheme of Fig. 6 with the results of Fig. 11 reproduces the essence of the complete quantum dynamical results shown in Fig. 13 of Ref. 168. The highly nonclassical “bistructural”

superposition state generated at  $t = 220$  ps introduces a fundamentally new concept in the history of molecular structure.<sup>170</sup> Such a state is at the same time a syn- and anti-isomer (like Schrödinger's cat would be assumed to be at the same time dead and alive) but it behaves very differently from a mixture of syn- and anti-structures, which would have time-independent spectra, for instance. Of course in terms of the concepts of classical molecular structures the quantum chameleon switch state would be considered impossible or "unphysical" (perhaps "unchemical"), but it is a perfectly real time-dependent quantum state and can be used, in principle, for quantum technology, quantum machines or quantum computing<sup>168,171</sup> opening thus opportunities going far beyond the possibilities of quasi-classical molecular switches and molecular machines.<sup>172</sup> We note here that the pulse sequence with  $\nu_{L1}$  and  $\nu_{L2}$  in the scheme allows, of course, also the realization of a quasi-classical molecular switch based on m-D-phenol and we refer to Ref. 168 for a more detailed discussion. We should mention also the considerations on the possible role of quasi-classical or quantum molecular switches in primary processes connected to the neurophysiology of vision and thought.<sup>52,56</sup>

### 3.4 Relaxation processes in multistate systems at high densities of states

Of course the simple scheme of Fig. 6 describes only certain special systems with well localized interactions in a realistic manner. In many real molecular primary processes one has to consider multistate interactions and interactions with (quasi-)continua. In the limit of high densities of states one will then observe kinetic relaxation phenomena as summarized schematically in Fig. 12.

The observation of relaxation processes after symmetry selective radiative excitation will provide access to the observation of a variety of primary processes related to symmetry breakings. The nature of these relaxation processes can be of different kinds and we refer to the detailed discussion of different statistical-mechanical cases in Refs. 46, 106, 108. In complex multilevel situations a complete analysis can be difficult, with sometimes ambiguous outcome. For instance, some of the slow relaxation processes in the IR-multiphoton excitation of  $^{12,13}\text{CF}_3\text{I}$  may be due to nuclear spin symmetry effects, but proof of this has not been possible, yet.<sup>173</sup> Complete relaxation of this kind at longer times would, however, be consistent also with the observation of statistical distributions of hyperfine levels in the iodine atom product of the dissociation of  $\text{CF}_3\text{I}$  after IR-multiphoton excitation.<sup>137,174</sup>

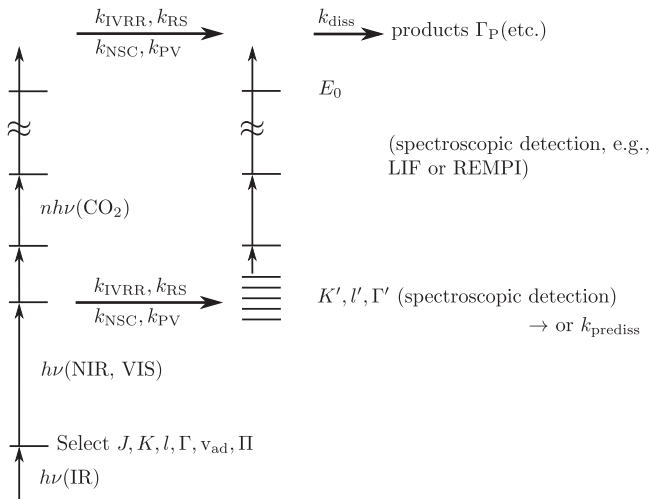
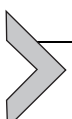


**Fig. 12** Selection of nuclear spin symmetry, parity, and other (approximately) conserved quantum numbers for kinetic detection of symmetry violations in polyatomic molecules. Rate constants describe nuclear spin conversion ( $k_{\text{NSC}}$ ), parity violation ( $k_{\text{PV}}$ ), stereomutation ( $k_{\text{RS}}$ ), intramolecular vibrational (rotational) redistribution ( $k_{\text{IVRR}}$ ), and dissociation ( $k_{\text{diss}}$ ). Modified after Quack, M. *Comments on the Role of Symmetries in Intramolecular Quantum Dynamics*. *Faraday Disc.* 1995, 102, 90–93, 358–360.



#### 4. The experimental approach toward parity violation in chiral molecules

The scheme of Fig. 6 for the preparation of exotic superposition states was originally proposed for fundamental investigations on chiral molecules, in particular also toward the observation of parity violation.<sup>46,47,175,176</sup> Within ordinary quantum chemistry retaining only the electromagnetic force (e.g., Refs. 53–55) the molecular Hamiltonian is strictly symmetric with respect to inversion of the spatial coordinates (parity operation  $\hat{P}$  or  $\hat{E}^*$ , with  $x \rightarrow -x$ ,  $y \rightarrow -y$ ,  $z \rightarrow -z$ ). Therefore one would have

$$\hat{P}\hat{H} = \hat{H}\hat{P} \quad (70)$$

This would be valid at all levels of accuracy and precision (including non-Born-Oppenheimer, relativistic, quantum electrodynamic effects, etc.). When including the weak (nuclear) force from the standard model of particle physics (SMPP) in the framework of what we have called “electroweak quantum chemistry,”<sup>79,130,177</sup> there is a small violation of space inversion symmetry with the consequence that we have

$$\hat{P}\hat{H}_{\text{ew}} \neq \hat{H}_{\text{ew}}\hat{P} \quad (71)$$

Whereas within ordinary “electromagnetic” quantum chemistry the reaction enthalpy  $\Delta_R H_0^\ominus$  for the stereomutation reaction (72) between enantiomers of chiral molecules would be exactly zero by symmetry which has been the assumption over the history of conventional stereochemistry,<sup>170</sup> as already noted by van’t Hoff, today’s electroweak quantum chemistry predicts a small “parity violating” energy difference  $\Delta_{\text{pv}}E$  between the ground states of the enantiomers

$$R \rightleftharpoons S \quad (72)$$

with

$$\Delta_R H_0^\ominus(\text{“electromagnetic”, van’t Hoff}) = 0 \quad (73)$$

or

$$\Delta_R H_0^\ominus(\text{“electroweak”}) = N_A \cdot \Delta_{\text{pv}}E \quad (74)$$

with the Avogadro constant  $N_A$ . The values for  $\Delta_{\text{pv}}E$  depend on the molecule. Current theory (reviewed in Refs. 3, 4, 130, 178, for example) predicts a typical order of magnitude in the sub-feV range (100 aeV to 1 feV), if chiral molecules containing only the lighter elements up to, say, Cl are included, larger values are possible when also heavier elements are involved.

Strictly speaking within parity conserving quantum mechanics at the time of Hund,<sup>38–40</sup> Eq. (70), the eigenstates of chiral molecules form tunneling doublets of well-defined parity for each state (+ or –) split by a tunneling splitting  $\Delta E_\pm$  related to the tunneling period  $\tau_{\text{RS}}$  for stereomutation

$$\tau_{\text{RS}} = h/\Delta E_\pm \quad (75)$$

Including parity violation one must distinguish two dynamical limiting cases.

**(i)** As long as  $\Delta_{\text{pv}}E$  is small compared to the tunneling splitting

$$\Delta_{\text{pv}}E \ll \Delta E_\pm \quad (76)$$

parity violation is unimportant and then rotation–vibration tunneling states retain their character with well-defined parity. This is applicable to molecules which are chiral in their equilibrium geometry but have a large tunneling splitting such as hydrogen peroxide HOOH<sup>74,75</sup> or ammonia NHDT,<sup>76</sup> with tunneling splittings on the order of  $\text{cm}^{-1}$  or, say,  $1 \text{ meV} \simeq (hc) \cdot 8 \text{ cm}^{-1}$ . Such molecules are only transiently chiral on the picosecond time scale.

**(ii)** On the other hand when parity violation dominates over tunneling

$$\Delta_{\text{pv}}E \gg \Delta E_\pm \quad (77)$$

the ground states have well localized chiral structures separated by an energy difference  $\Delta_{\text{pv}}E$ . This case actually applies to molecules that exist as stable enantiomers under normal conditions such as CHFCIBr.<sup>81,179,228</sup>

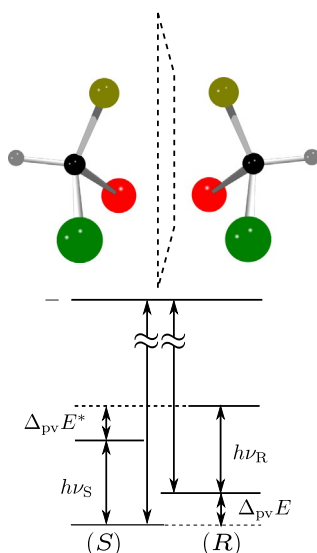


**Fig. 13** The energies of the S and R enantiomers are different due to symmetry violation, note:  $h\nu_R - h\nu_S = \Delta_{pv}E^* - \Delta_{pv}E$ . Modified after Quack, M.; Stohner, J. Influence of Parity Violating Weak Nuclear Potentials on Vibrational and Rotational Frequencies in Chiral Molecules. *Phys. Rev. Lett.* 2000, 84 (17), 3807–3810; Quack, M. How Important Is Parity Violation for Molecular and Biomolecular Chirality? *Angew. Chem. Int. Edit.* 2002, 41, 4618–4630. *Angew. Chem.* 2002, 114, 4812–4825.

**Fig. 13** shows the energy level scheme for such molecules. Even for molecules with rather modest barriers for stereomutation such as ClSSCl with a barrier of about  $6000\text{ cm}^{-1}$ , tunneling splittings for the hypothetical symmetric case are exceedingly small with hypothetical tunneling times much exceeding the age of the universe.<sup>77</sup>

Therefore the condition Eq. (77) is frequently satisfied and  $\Delta_{pv}E$  is a measurable energy difference between isomers, as we had also discussed for the achiral molecule m-D-phenol in [Section 3](#). The new aspect is the exceedingly small magnitude of  $\Delta_{pv}E$  (100 aeV for CHFClBr<sup>81,179,228</sup> corresponds to about  $10^{-11}\text{ J mol}^{-1}$  or  $10^{-12}\text{ cm}^{-1}$ ) as compared to other isomerization energies (say  $(hc) \cdot 0.8\text{ cm}^{-1}$  for syn- and anti- m-D-phenol, considered already to be quite a small value). Therefore a spectroscopic analysis with the ordinary techniques of high-resolution spectroscopy as for m-D-phenol discussed in [Section 3.3](#) cannot be successful (note the 12 orders of magnitude jump).

There have been a number of proposals for special techniques to measure  $\Delta_{pv}E$  reviewed in Ref. 3 in more detail. We had mentioned already the level crossing experiment discussed in Ref. 162 in [Section 3.3](#). As of today there seem to be only two major efforts world wide, one in Zurich which started with first publications in 1986<sup>46,47</sup> and one in Paris starting with first

publications in 1999.<sup>180</sup> The two projects have been reviewed for example in Refs. 3, 4, 131, 181, 219 and we shall not discuss details.

We note, however, the basic difference of the approaches. In the approach from Paris (Ref. 180 following an earlier suggestion of Letokhov<sup>182</sup> and related spectroscopic work preparing for such experiments in Zurich<sup>62,183,229</sup>) one measures at ultrahigh precision the absorption lines in infrared spectra of separate enantiomers  $\hbar\nu_R$  and  $\hbar\nu_S$  in Fig. 13, which then would provide a difference of parity violating energy differences

$$\Delta_{\text{pv}}E^* - \Delta_{\text{pv}}E = h(\nu_R - \nu_S) \quad (78)$$

So far these experiments have not been successful, but with current developments of high-resolution techniques one can hope for success in the future for molecules with very large  $\Delta_{\text{pv}}E$  (when containing very heavy elements).

Our approach in Zurich uses the idea of the scheme in Fig. 6. At high internal excitations the tunneling splittings may become large enough such that

$$\Delta E_{\pm}^{**} \gg \Delta_{\text{pv}}E^{**} \quad (79)$$

for some excited level (a typical “tunneling switching” situation). Or else one can use rovibrational levels of well-defined parity in an excited electronic state which is achiral, for instance planar as illustrated in Fig. 14.

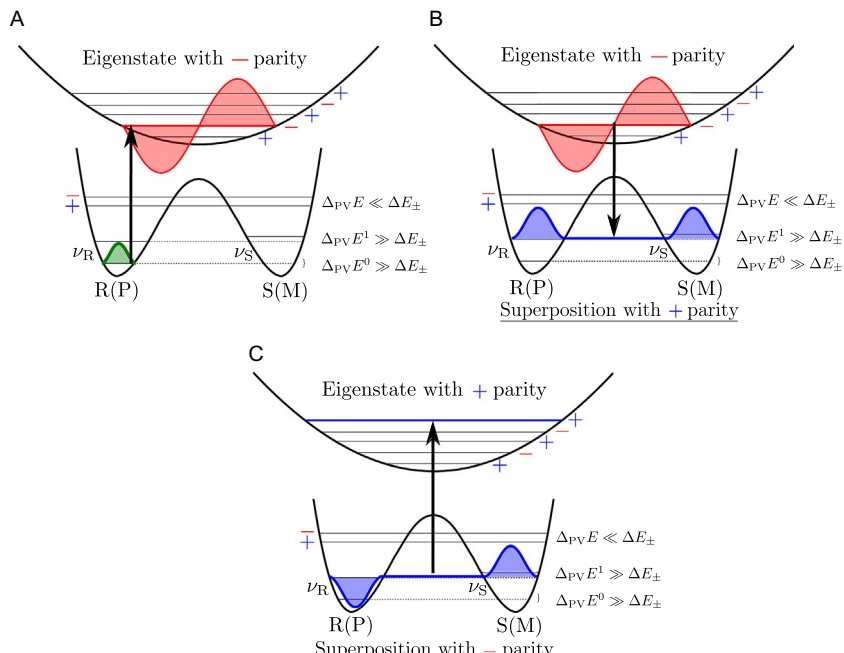


**Fig. 14** Generation of a superposition state with initially + parity and probing for the opposite – parity using ground and excited electronic states.

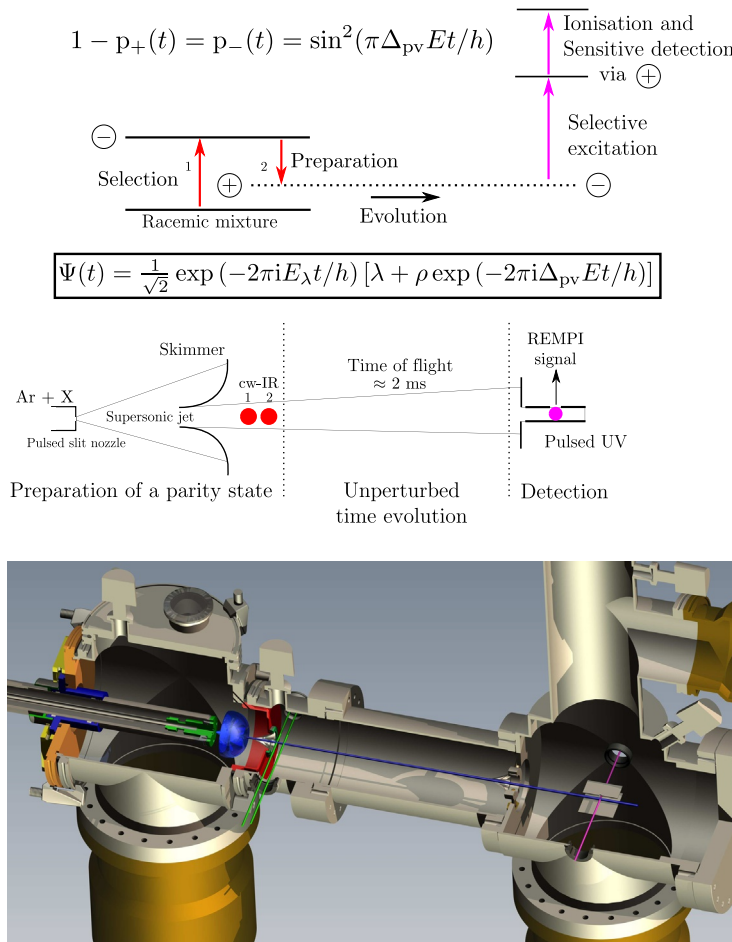


**Fig. 15** Experimental molecular beam setup showing the three laser beams of the three steps. Modified after Dietiker, P.; Miloglyadov, E.; Quack, M.; Schneider, A.; Seyfang, G. Infrared Laser Induced Population Transfer and Parity Selection in  $^{14}\text{NH}_3$ : A Proof of Principle Experiment Towards Detecting Parity Violation in Chiral Molecules. *J. Chem. Phys.* 2015, 143 (24), 244305.

Alternatively as also sketched in Fig. 14 one can use an excited tunneling doublet in the electronic ground state, satisfying Eq. (79). Fig. 15 shows a schematic representation of the several steps. Among the advantages of this approach one can recall that it allows for a separate measurement of individual  $\Delta_{pv}E$ ,  $\Delta_{pv}E^*$ , etc, not only differences of differences. It also does not need enantiopure samples, one could work on racemic mixtures as starting

materials. Furthermore for the selection and preparation steps one needs a typical frequency resolution in the MHz range only.

Nevertheless, with an evolution time in the ms time range provided by a flight path in a molecular beam setup (Fig. 15) of about 1 m we have demonstrated that with sensitive detection by multiphoton ionization on the test molecule NH<sub>3</sub> we could achieve a sensitivity which would correspond to a measurement of a  $\Delta_{\text{pv}}E$  of about 100 aeV in a chiral molecule.<sup>83</sup> Obviously, NH<sub>3</sub> is not chiral and thus the experiment demonstrates effectively parity conservation for the spectroscopic parity states.

$\Delta_{\text{pv}}E$  of 100 aeV and even larger values exist for molecules involving only elements lighter than Cl or S,<sup>3,82,131,169,184,186,191</sup> which is an advantage in the theoretical analysis. Fig. 16 illustrates schematically the spectral changes and provides a nice illustration for our motivation to call such time-dependent “parity isomers” a “quantum chameleon” changing color. While showing the same quantum characteristic as a Schrödinger cat, the molecular quantum chameleon as animal analogy stays alive in the experiment and only changes color “while being exposed to mild forms of harmless infrared radiation.”<sup>52</sup>

Fig. 17 finally illustrates the steps in the experiment with a realistic simulation for the molecule ClOOCl.<sup>82</sup> This follows in essence the steps Laser 1 ( $\nu_{L1}$ ) and Laser 3 ( $\nu_{L3}$ ) in the scheme of Fig. 6 but the simulations are for a realistic theoretical and quantum dynamical representation

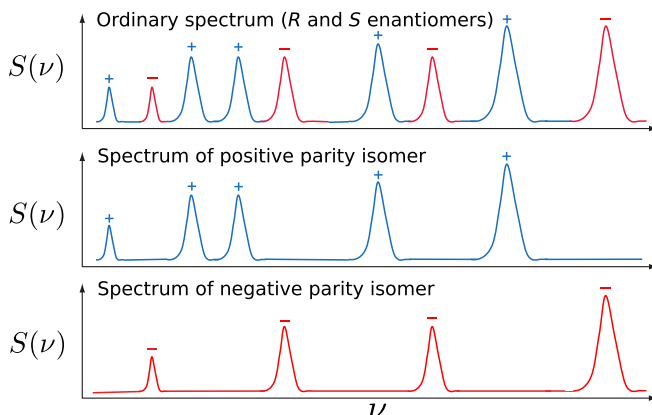


**Fig. 16** Schematic illustration of the spectral changes in the superposition experiment. Modified after Quack, M. On Biomolecular Homochirality as a Quasi-Fossil of the Evolution of Life. *Adv. Chem. Phys.* 2014, 157, 249–290.

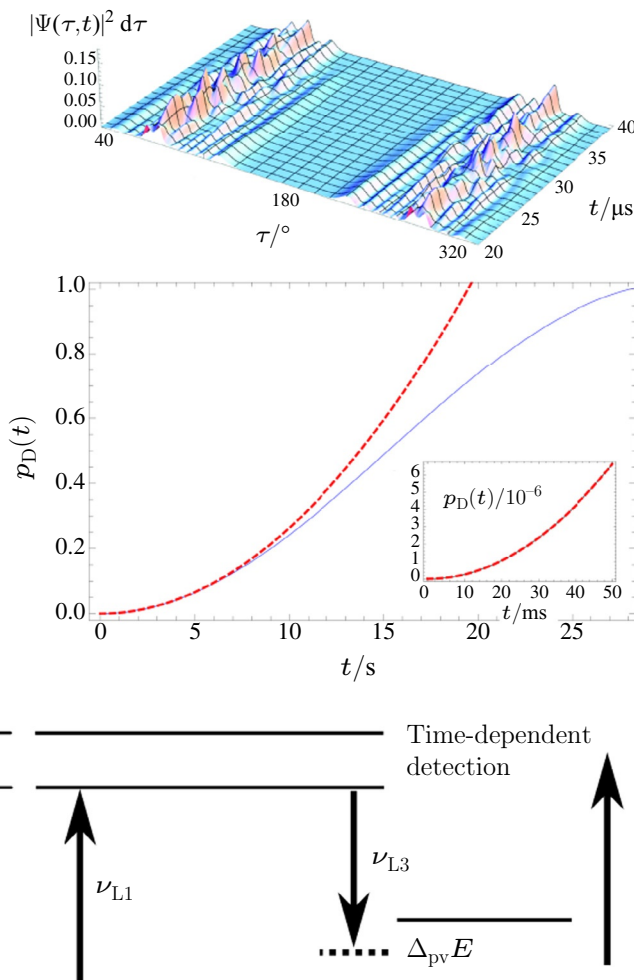


**Fig. 17** The upper part shows the time-dependent wavepacket (as probability  $|\Psi(\tau, t)|^2$   $d\tau$ ) as a function of the torsion angle  $\tau$ , integrated over all other coordinates in ClOOCl) during the transfer process shown for  $20 \mu\text{s} \leq t \leq 40 \mu\text{s}$  with  $d\tau = \Delta\tau = 1^\circ$ . The delocalized wavepacket generated after the pump pulse becomes a wavepacket of a superposition state  $\chi$  with initially well-defined parity (at  $t \approx 40 \mu\text{s}$ ) after using a frequency-modulated transfer pulse. At much longer times ( $t > 1 \text{ ms}$ ); however, the parity is time-dependent leading to nonzero detection probability,  $p_D(t)$  for parity change (shown in the middle part). At the bottom the simplified level scheme is shown. Modified after Prentner, R.; Quack, M.; Stohner, J.; Willeke, M. Wavepacket Dynamics of the Axially Chiral Molecule Cl-O-O-Cl under Coherent Radiative Excitation and Including Electroweak Parity Violation. *J. Phys. Chem. A* 2015, 119 (51), 12805–12822.

of a real molecule, where for the first time vibration–rotation–tunneling dynamics, coherent radiative excitation and electroweak parity violation were included in the computations.<sup>82</sup> The major current challenge concerns the analysis of the very complex tunneling–rotation–vibration spectra of suitable chiral molecules that could be used for these experiments.<sup>4,184–186</sup>



## 5. Concluding remarks on theory, experiment, and future possibilities

Symmetry in chemistry is frequently associated with purely geometrical concepts.<sup>1,230,231</sup> The many facets of the symmetries of crystals with their beautiful shapes have a long and rich history.<sup>187,188</sup> This gives a purely static picture. Here we have addressed symmetry from a quantum dynamical and kinetic point of view.<sup>25,51</sup> The breaking of approximate symmetries and the time evolution of approximate constants of the motion provide a window on the time scales of many important processes. The experimental concept for the preparation and evolution of exotic superposition isomers offers opportunities for fundamental experiments, notably the measurement of the parity violating energy difference  $\Delta_{\text{pv}}E$  between enantiomers of chiral molecules,<sup>47</sup> but also for possible uses of molecular quantum switches in quantum technology and quantum information.<sup>168</sup> While the experiment to measure  $\Delta_{\text{pv}}E$  in chiral molecules might have appeared to be impossible, when it was first proposed,<sup>46,47,175</sup> the current outlook for a successful experiment is excellent. Indeed, provided that adequate funding for the continuation of the current project can be secured and that the required spectroscopic analyses thereby can be completed, most significant results for each of the possible outcomes of the experiment can be expected:

- (i) Either one finds in the experiment the theoretically predicted value for  $\Delta_{\text{pv}}E$ , then one can analyze the results of the precision experiments in terms of properties of the standard model of particle physics (SMPP) in a range of quantum systems not yet tested by previous experiments.<sup>3</sup>
- (ii) Or else, if one finds values for  $\Delta_{\text{pv}}E$  different from the theoretical predictions, this will lead to a fundamental revision of current theories for  $\Delta_{\text{pv}}E$  with even the potential for “new physics.”<sup>3</sup>

- (iii) Finally, a profound experimental and theoretical understanding of  $\Delta_{\text{pv}}E$  in chiral molecules can be a first step toward understanding the possible implications for our understanding of biomolecular homochirality.<sup>4,179,232</sup>

The underlying theoretical concept as well for the design of experiments as also for a quantitative theory is the study of the evolution of approximate constants of the motion discussed in Section 2. It allows us to separately and accurately determine the very small parity violating contributions in the Hamiltonian independent of any of the (large) uncertainties in the much larger contributions from the parity conserving “electromagnetic” Hamiltonian of ordinary quantum chemistry. Interestingly it also leads us to fundamental investigations at the “long time frontier” of the molecular primary processes summarized in Table 1. These parity violating processes happen on time scales of seconds, but they are induced by the Z-Boson as field particle, the lifetime of which appears at the current experimental short time frontier in physics in the subyocto second time range. Thus, indeed, the underlying physics of these processes connects primary processes ranging from the yoctosecond to the second time scale, and longer, if we also include the role of tunneling processes in chiral molecules.<sup>25,44,45</sup>

Some brief remarks may be in order concerning the current status of the theory of parity violation in chiral molecules, which has been reviewed in detail elsewhere<sup>3,130,131,178,189,190</sup> (see also Refs. 1, 79, 157, 191). The history of this theory can be broadly summarized in three phases. In a first phase after discovery of parity violation in nuclear and high energy physics<sup>192–197</sup> in 1957, qualitative suggestions were made concerning the role of parity violation in chiral molecules, with estimates which were often wrong by many orders of magnitude (in the period of about 1960–80,<sup>233–235</sup> see also the reviews in Refs. 1, 3, 46, 130). Attempts toward a quantitative theory started in about 1980 based in particular on the work of Hegström, Rein and Sandars,<sup>198</sup> Mason, and Tranter,<sup>199</sup> and others<sup>200,201</sup> (see also the reviews<sup>3,130,131,157</sup>). It turned out, however, that these approaches were quantitatively inadequate. When we carefully reinvestigated the theory starting from its foundations in the standard model and critically analyzed the effects within “electroweak” quantum chemistry,<sup>79,80,177</sup> we found in 1993–95 values for  $\Delta_{\text{pv}}E$  by one and often two orders of magnitude larger for typical benchmark molecules as compared to previous results. These new values were subsequently confirmed by quite a few other theory groups,<sup>202–205</sup> (see the reviews in Refs. 3, 130, 131, 157, 178 for much more

complete references). Today there seems to be general agreement from different approaches on the new orders of magnitude (see for instance the recent summary in Ref. 191). One may thus assume, that at least no “trivial” effects have been overlooked in the theories.

Nevertheless, given the earlier history, experimental tests seem to be an absolute requirement. The new orders of magnitude have also made the outlook for such experiments much more promising.

We may conclude here with an outlook on new frontiers in experiment in the more distant future. Time reversal symmetry violation is a topic of interest. Some experiments attempt the measurement of a permanent electric dipole moment of electrons in this context, also for diatomic molecules<sup>206,207</sup> (see also the reviews in Refs. 1, 3, 190). A more direct molecular alternative would be “motion reversal” in a polyatomic molecule, say, by a sequence of laser pulses, which amounts to seeing entropy reversal.<sup>87,101,157</sup> So far there is neither a successful experiment nor a quantitative theory available for such an effect in molecules, but the effect is known in particle physics.<sup>208</sup> Clearly, looking at the lower part of Table 1 in Section 2 the most challenging frontier would be a test of CPT symmetry, the simultaneous inversion of charge (C for charge conjugation), parity (P representing space inversion) and time (T for time reversal). Current tests using the mass of the proton compared to the antiproton have tested this symmetry at a precision of about  $10^{-12}$  (for  $\Delta m/m$  in the masses<sup>206</sup>). A similar precision has been reached very recently in studies of the spectrum of hydrogen atom in comparison with antihydrogen.<sup>209</sup> These latter approaches should, however, be extendable to a precision of  $10^{-18}$  with current spectroscopic technology.<sup>236,237</sup> About this level of precision and even better has also been reached for leptonic matter (when measuring the g-values of the electron and positron<sup>210–212</sup>). A CPT test with a precision of  $10^{-19}$  has been claimed in studies of the neutral K-meson (Kaon), the nature of the test being somewhat different from the other tests mentioned (see also Ref. 238).<sup>213</sup>

We have shown, that using the spectroscopic concept of the exotic superposition of molecular isomers one might be able to reach a precision corresponding to  $\Delta m/m \approx 10^{-30}$ , by essentially the experimental approach described in Section 4 (then on hypothetical chiral clusters of antihydrogen<sup>49,51,85,214</sup>). While this is not expected to be feasible in the near future, it demonstrates the power of the experimental concept. Fig. 18 provides a brief graphical summary of such a scheme involving matter and antimatter.<sup>3,51,85</sup> We might note here even the recent extensions to theoretical

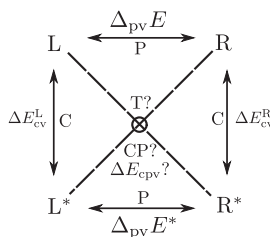


**Fig. 18** Stereochemistry and CPT—symmetry (violation). Modified after Quack, M. Molecular Quantum Dynamics from High-Resolution Spectroscopy and Laser Chemistry. *J. Mol. Struct.* 1993, 292, 171–195; Quack, M. On the Measurement of CP-Violating Energy Differences in Matter-Antimatter Enantiomers. *Chem. Phys. Lett.* 1994, 231, 4–6.

studies in cosmology as far fetched as this may seem.<sup>215</sup> We might mention as well, that, in principle, the preparation and observation of the “exotic superpositions” of the enantiomers of chiral molecules or other, more complex objects based on this technique could be considered to be a fundamental test of the superposition principle of quantum mechanics which can also be related to the neurophysiology of vision and thought, so far hypothetical.<sup>56</sup>

## Acknowledgments

We are very grateful to Kenneth Ruud for the hospitality extended at the Tromsø2019 conference and to Erkki Brändas for correspondence and for his patience in waiting for our chapter. Our work has profited from discussions and continuous support from Frédéric Merkt and from substantial financial support from an ERC Advanced Grant on this subject matter as well as from ETH Zürich grants. Numerous coworkers have contributed importantly of whom we should highlight recent coworkers notably Sieghard Albert, Ziqiu Chen, Csaba Fabri, Karen Keppler, Roberto Marquardt, Eduard Miloglyadov, Andreas Schneider, Jürgen Stohner, Martin Willeke, and Daniel Zindel. Further important contributions can be seen from the list of references and the lists given in Refs. 51 and 216. We also acknowledge discussions and correspondence with Harald Fritzsch, Peter Jenni, Felicitas Pauss, and Herwig Schopper on the SMPP, Z, and Higgs Bosons and support from the COST project MOLIM. This publication as the session in Tromsø2019 is dedicated to the memory of Janos Ladik.

## References

1. Symmetrie und Asymmetrie in Wissenschaft und Kunst. In *Nova Acta Leopoldina NF* 127, Nr. 412; Quack, M., Hacker, J., Eds.; Wissenschaftliche Verlagsgesellschaft, Stuttgart, 2016 (Book with contributions in German and English from several authors).
2. Quack, M. Detailed Symmetry Selection-Rules for Reactive Collisions. *Mol. Phys.* **1977**, *34*(2), 477–504.
3. Quack, M. Fundamental Symmetries and Symmetry Violations From High Resolution Spectroscopy. In *Handbook of High Resolution Spectroscopy*; Quack, M., Merkt, F., Eds.; Vol. 1, Wiley: Chichester, New York, 2011; pp 659–722. (Chapter 18).

4. Quack, M. On Biomolecular Homochirality as a Quasi-Fossil of the Evolution of Life. *Adv. Chem. Phys.* **2014**, *157*, 249–290.
5. Wilhelmy, L. Ueber das Gesetz, nach welchem die Einwirkung der Säuren auf den Rohrzucker stattfindet. *Poggendorff's Annalen der Physik* **1850**, *81*(11), 413–428, 499–526 (Reprinted in Ostwalds Klassiker, also vol. *157*, Ann. der Physik).
6. Eigen, M. Paracelsus Prize Lecture. *Chimia* **1968**, *22*, 310.
7. Eigen, M. Die unmessbar schnellen Reaktionen. *Ostwalds Klassiker der exakten Wissenschaften*; Vol. 281, Verlag Harri Deutsch: Thun and Frankfurt, 1996.
8. Porter, G. Flash Photolysis into the Femtosecond—A Race Against Time. In *Femtosecond Chemistry*; Manz, J., Wöste, L., Eds.; VCH Publ. Weinheim, 1995; pp 3–13. (Chapter 1).
9. Troe, J. Shock wave studies of elementary chemical processes. *Modern Developments in Shock Tube Research, Proc. 10th. Int. Shock Tub. Symp. Kyoto*; Shock tube Res. Soc, 1975; pp 29–54.
10. Green, E. F.; Toennies, J. P. *Chemische Reaktionen in Stosswellen*. Steinkopff Verlag: Darmstadt, 1959.
11. Fleming, G. *Chemical Applications of Ultrafast Spectroscopy*. Oxford University Press: Oxford, 1986.
12. Zewail, A. H. Femtochemistry: Concepts and Applications. In *Femtosecond Chemistry*; Manz, J., Wöste, L., Eds.; VCH Publ. Weinheim, 1995; pp 14–128. (Chapter 2).
13. Kraus, F. Tracking Light Oscillations: Attosecond Spectroscopy Comes of Age. *Opt. Photon. News* **2002**, *13*, 62–68.
14. Wörner, H. J.; Corkum, P. Attosecond Spectroscopy. In *Handbook of High-Resolution Spectroscopy*; Quack, M., Merkt, F., Eds.; Vol. 3, Wiley: Chichester, New York, 2011; pp 1781–1804.
15. Gallmann, L.; Keller, U. Femtosecond and Attosecond Light Sources and Techniques for Spectroscopy. In *Handbook of High-Resolution Spectroscopy*; Quack, M., Merkt, F., Eds.; Vol. 3, Wiley: Chichester, New York, 2011; pp 1805–1836.
16. Lee, Y. T. Molecular Beam Studies of Elementary Chemical Processes (Nobel Lecture). *Angew. Chem. Intl. Ed.* **1987**, *26*, 939–951.
17. Faubel, M.; Toennies, J. P. Scattering Studies of Rotational and Vibrational Excitation of Molecules. *Adv. Atom. Mol. Phys.* **1978**, *13*, 229–314.
18. Levine, R. D.; Bernstein, R. B. *Molecular Reaction Dynamics and Chemical Reactivity*. Oxford University Press: Oxford, 1986.
19. Zare, R. N. Polanyi Memorial Lecture. *Faraday Discuss. Chem. Soc.* **1979**, *67*, 7–15.
20. Crim, F. F. Bond-Selected Chemistry: Vibrational State Control of Photodissociation and Bimolecular Reaction. *J. Phys. Chem.* **1996**, *100*(31), 12725–12734.
21. Ernst, R. R.; Bodenhausen, G.; Wokaun, A. *Principles of Nuclear Magnetic Resonance in One and Two Dimensions*. Clarendon Press: Oxford, 1997.
22. Schweiger, A.; Jeschke, G. *Principles of Pulse Electron Paramagnetic Resonance*. Oxford University Press: Oxford, 2001.
23. Knox, W. H.; Knox, R. S.; Hoose, J. F.; Zare, R. N. Observation of the 0-fs Pulse. *Opt. Photon. News* **1990**, *1*, 44–45.
24. Ullrich, J.; Moshammer, R.; Dörner, R. Ein ‘Attosekunden-Mikroskop?’ *Phys. Bl.* **1998**, *54*(2), 140–143.
25. Quack, M. Molecular Femtosecond Quantum Dynamics Between Less Than Yoctoseconds and More than Days: Experiment and Theory. In *Femtosecond Chemistry, Proc. Berlin Conf. Femtosecond Chemistry, Berlin (March 1993)*; Manz, J., Wöste, L., Eds.; Verlag Chemie: Weinheim, 1995; pp 781–818. (Chapter 27).
26. Troe, J. Reaction Kinetics: An Addiction. *J. Phys. Chem. A* **2006**, *110*(9), 2831–2834.
27. Jortner, J. Unended Quest in Science. *Isr. J. Chem.* **2003**, *43*(3–4), 169–217.

28. Marquardt, R.; Quack, M. *Molecular Spectroscopy and Quantum Dynamics*. Elsevier: Amsterdam, 2020; see also preface and chapter 1 therein (in press).
29. Merkt, F.; Quack, M. Molecular Quantum Mechanics and Molecular Spectra, Molecular Symmetry, and Interaction of Matter With Radiation. In *Handbook of High-Resolution Spectroscopy*; Quack, M., Merkt, F., Eds.; Vol. 1, Wiley: Chichester, New York, 2011; pp 1–55. (Chapter 1).
30. Schrödinger, E. Quantisierung als Eigenwertproblem IV. *Ann. Phys.* **1926**, *81*, 109–139.
31. Schrödinger, E. Quantisierung als Eigenwertproblem I. *Ann. Phys.* **1926**, *79*, 361–376.
32. Schrödinger, E. Quantisierung als Eigenwertproblem II. *Ann. Phys.* **1926**, *79*, 489–527.
33. Schrödinger, E. Quantisierung als Eigenwertproblem III. *Ann. Phys.* **1926**, *80*, 437–490.
34. Schrödinger, E. Der stetige Übergang von der Mikro zur Makro Mechanik. *Naturwissenschaften* **1926**, *14*, 664–666.
35. Heisenberg, W. Über quantentheoretische Umdeutung kinematischer und mechanischer Beziehungen. *Z. Phys.* **1926**, *33*, 879–893.
36. Heisenberg, W. *Die Physikalischen Prinzipien der Quantentheorie*. Hirzel Verlag: Leipzig, 1980.
37. Dirac, P. A. M. *The Principles of Quantum Mechanics*, 4th ed.; Clarendon Press: Oxford, 1958.
38. Hund, F. Symmetriecharaktere von Termen bei Systemen mit gleichen Partikeln in der Quantenmechanik. *Z. Phys.* **1927**, *43*, 788–804.
39. Hund, F. Zur Deutung der Molekelspektren. III., Bemerkungen über das Schwingungs- und Rotationsspektrum bei Molekülen mit mehr als zwei Kernen. *Z. Phys.* **1927**, *43*, 805–826.
40. Hund, F. Zur Deutung der Molekelspektren. I. *Z. Phys.* **1927**, *40*, 742–764.
41. Wentzel, G. Über strahlunglose Quantensprünge. *Z. Phys.* **1927**, *43*, 524–530.
42. Bixon, M.; Jortner, J. Intramolecular Radiationless Transitions. *J. Chem. Phys.* **1968**, *48*(2), 715–726.
43. Miller, W. H. A Journey Through Chemical Dynamics. *Ann. Rev. Phys. Chem.* **2014**, *65*(1), 1–19.
44. Seyfang, G.; Quack, M. Atomare und Molekulare Tunnelprozesse. *Nachr. Chem.* **2018**, *66*, 307–315.
45. Quack, M.; Seyfang, G. Atomic and Molecular Tunneling Processes. In *Molecular Spectroscopy and Quantum Dynamics*; Marquardt, R., Quack, M., Eds.; Elsevier: Amsterdam, 2020; (in press).
46. Quack, M. Structure and Dynamics of Chiral Molecules. *Angew. Chem. Int. Edit.* **1989**, *28*(5), 571–586. *Angew. Chem.*, **1989**, *101*, 588–604.
47. Quack, M. On the Measurement of the Parity Violating Energy Difference Between Enantiomers. *Chem. Phys. Lett.* **1986**, *132*(2), 147–153.
48. Quack, M. Spectra and Dynamics of Coupled Vibrations in Polyatomic Molecules. *Ann. Rev. Phys. Chem.* **1990**, *41*, 839–874.
49. Quack, M. Molecular Quantum Dynamics from High-Resolution Spectroscopy and Laser Chemistry. *J. Mol. Struct.* **1993**, *292*, 171–195.
50. Quack, M. Molecules in Motion. *Chimia* **2001**, *55*, 753–758.
51. Quack, M. Molecular Spectra, Reaction Dynamics, Symmetries and Life. *Chimia* **2003**, *57*(4), 147–160.
52. Quack, M. *Telluride Public Lecture*, Telluride. 1995. Unpublished, in part contained in Ref. 56.
53. Reiher, M.; Wolf, A. *Relativistic Quantum Chemistry, The Fundamental Theory of Molecular Science*, 1st ed.; Wiley VCH Weinheim, 2009.
54. Helgaker, T.; Jorgensen, P.; Olsen, J. *Molecular Electronic-Structure Theory*. Wiley, 2014.
55. Schaefer, H. F., III *Quantum Chemistry: The Development of Ab Initio Methods in Molecular Electronic Structure Theory*. Oxford University Press: Oxford, 1984.

56. Quack, M. Time and Time Reversal Symmetry in Quantum Chemical Kinetics. In *Fundamental World of Quantum Chemistry. A Tribute to the Memory of Per-Olov Löwdin*; Brändas, E. J., Kryachko, E. S., Eds.; Vol. 3, Kluwer Academic Publishers: Dordrecht, 2004; pp 423–474.
57. Quack, M. Comments on the Role of Symmetries in Intramolecular Quantum Dynamics. *Faraday Disc.* **1995**, *102*, 90–93, 358–360.
58. Dübal, H. R.; Quack, M. Tridiagonal Fermi Resonance Structure in the IR-Spectrum of the Excited CH Chromophore in CF<sub>3</sub>CH. *J. Chem. Phys.* **1984**, *81*(9), 3779–3791.
59. Marquardt, R.; Quack, M.; Stohner, J.; Sutcliffe, E. Quantum-Mechanical Wavepacket Dynamics of the CH Group in Symmetric Top X<sub>3</sub>CH Compounds Using Effective-Hamiltonians from High-Resolution Spectroscopy. *J. Chem. Soc. Farad. Trans. 2* **1986**, *82*, 1173–1187.
60. Marquardt, R.; Quack, M. The Wave Packet Motion and Intramolecular Vibrational Redistribution in CHX<sub>3</sub> Molecules Under Infrared Multiphoton Excitation. *J. Chem. Phys.* **1991**, *95*(7), 4854–4876.
61. Quack, M.; Stohner, J. Femtosecond Quantum Dynamics of Functional-Groups Under Coherent Infrared Multiphoton Excitation as Derived From the Analysis of High-Resolution Spectra. *J. Phys. Chem.* **1993**, *97*(48), 12574–12590.
62. Beil, A.; Luckhaus, D.; Quack, M. Fermi Resonance Structure and Femtosecond Quantum Dynamics of a Chiral Molecule From the Analysis of Vibrational Overtone Spectra of CHBrClF. *Ber. Bunsenges. Phys. Chem.* **1996**, *100*(11), 1853–1875.
63. Beil, A.; Hollenstein, H.; Monti, O. L. A.; Quack, M.; Stohner, J. Vibrational Spectra and Intramolecular Vibrational Redistribution in Highly Excited Deuterobromochlorofluoromethane CDBrClF: Experiment and Theory. *J. Chem. Phys.* **2000**, *113*(7), 2701–2718.
64. Pochert, J.; Quack, M.; Stohner, J.; Willeke, M. Ab Initio Calculation and Spectroscopic Analysis of the Intramolecular Vibrational Redistribution in 1,1,1,2-Tetrafluoroiodoethane CF<sub>3</sub>CHFI. *J. Chem. Phys.* **2000**, *113*(7), 2719–2735.
65. He, Y. B.; Hollenstein, H.; Quack, M.; Richard, E.; Snels, M.; Bürger, H. High Resolution Analysis of the Complex Symmetric CF<sub>3</sub> Stretching Chromophore Absorption in CF<sub>3</sub>I. *J. Chem. Phys.* **2002**, *116*(3), 974–983.
66. Albert, S.; Keppler Albert, K.; Hollenstein, H.; Manca Tanner, C.; Quack, M. Fundamentals of Rotation-Vibration Spectra. In *Handbook of High-Resolution Spectroscopy*; Quack, M., Merkt, F., Eds.; Vol. 1, Wiley: Chichester, New York, 2011; pp 117–173. (Chapter 3).
67. Albert, S.; Bekhtereva, E.; Bolotova, I.; Chen, Z.; Fábris, C.; Hollenstein, H.; Quack, M.; Ulenikov, O. Isotope Effects on the Resonance Interactions and Vibrational Quantum Dynamics of Fluoroform <sup>12</sup>, <sup>13</sup>CHF<sub>3</sub>. *Phys. Chem. Chem. Phys.* **2017**, *19*, 26527–26534.
68. von Puttkamer, K.; Dübal, H. R.; Quack, M. Time-Dependent Processes in Polyatomic-Molecules During and after Intense Infrared Irradiation. *Faraday Disc.* **1983**, *75*, 197–210.
69. Quack, M.; Suhm, M. A. Potential Energy Surfaces, Quasi-Adiabatic Channels, Rovibrational Spectra, and Intramolecular Dynamics of (HF)<sub>2</sub> and Its Isotopomers from Quantum Monte Carlo Calculations. *J. Chem. Phys.* **1991**, *95*(1), 28–59.
70. von Puttkamer, K.; Quack, M. Vibrational Spectra of (HF)<sub>2</sub>, (HF)<sub>n</sub> and their D-Isotopomers – Mode Selective Rearrangements and Nonstatistical Unimolecular Decay. *Chem. Phys.* **1989**, *139*(1), 31–53.
71. Hippler, M.; Oeltjen, L.; Quack, M. High-Resolution Continuous-Wave-Diode Laser Cavity Ring-Down Spectroscopy of the Hydrogen Fluoride Dimer in a Pulsed Slit Jet Expansion: Two Components of the N = 2 Triad Near 1.3 micrometer. *J. Phys. Chem. A* **2007**, *111*(49), 12659–12668.

72. Kushnarenko, A.; Miloglyadov, E.; Quack, M.; Seyfang, G. Intramolecular vibrational Energy Redistribution in HCCCH<sub>2</sub>X (X = Cl, Br, I) Measured by Femtosecond Pump-Probe Experiments in a Hollow Waveguide. *Phys. Chem. Chem. Phys.* **2018**, *20*, 10949–10959.
73. Luckhaus, D.; Quack, M. The Role of Potential Anisotropy in the Dynamics of the CH-Chromophore in CHX<sub>3</sub> (C<sub>3v</sub>) Symmetrical Tops. *Chem. Phys. Lett.* **1993**, *205*(2–3), 277–284.
74. Fehrensen, B.; Luckhaus, D.; Quack, M. Mode Selective Stereomutation Tunnelling in Hydrogen Peroxide Isotopomers. *Chem. Phys. Lett.* **1999**, *300*(3–4), 312–320.
75. Fehrensen, B.; Luckhaus, D.; Quack, M. Stereomutation Dynamics in Hydrogen Peroxide. *Chem. Phys.* **2007**, *338*(2–3), 90–105.
76. Fábri, C.; Marquardt, R.; Császár, A.; Quack, M. Controlling Tunneling in Ammonia Isotopomers. *J. Chem. Phys.* **2019**, *150*, 014102.
77. Berger, R.; Gottselig, M.; Quack, M.; Willeke, M. Parity Violation Dominates the Dynamics of Chirality in Dichlorodisulfane. *Angew. Chem. Int. Edit.* **2001**, *40*(22), 4195–4198. *Angew. Chem.* **2001**, *113*, 4342–4345.
78. Chapovsky, P. L.; Hermans, L. J. F. Nuclear Spin Conversion in Polyatomic Molecules. *Ann. Rev. Phys. Chem.* **1999**, *50*(1), 315–345. <https://doi.org/10.1146/annurev.physchem.50.1.315>.
79. Bakasov, A.; Ha, T. K.; Quack, M. Ab Initio Calculation of Molecular Energies Including Parity Violating Interactions. *J. Chem. Phys.* **1998**, *109*(17), 7263–7285.
80. Berger, R.; Quack, M. Multiconfiguration Linear Response Approach to the Calculation of Parity Violating Potentials in Polyatomic Molecules. *J. Chem. Phys.* **2000**, *112*(7), 3148–3158.
81. Quack, M.; Stohner, J. Influence of Parity Violating Weak Nuclear Potentials on Vibrational and Rotational Frequencies in Chiral Molecules. *Phys. Rev. Lett.* **2000**, *84*(17), 3807–3810.
82. Prentner, R.; Quack, M.; Stohner, J.; Willeke, M. Wavepacket Dynamics of the Axially Chiral Molecule Cl-O-O-Cl under Coherent Radiative Excitation and Including Electroweak Parity Violation. *J. Phys. Chem. A* **2015**, *119*(51), 12805–12822.
83. Dietiker, P.; Miloglyadov, E.; Quack, M.; Schneider, A.; Seyfang, G. Infrared Laser Induced Population Transfer and Parity Selection in <sup>14</sup>NH<sub>3</sub>: A Proof of Principle Experiment Towards Detecting Parity Violation in Chiral Molecules. *J. Chem. Phys.* **2015**, *143*(24), 244305.
84. Miloglyadov, E.; Quack, M.; Seyfang, G.; Wichmann, G. Precision Experiments for Parity Violation in Chiral Molecules: The Role of STIRAP. *J. Phys. B At. Mol. Opt. Phys.* **2019**, *52*, ch. A2.3, 11–13 and 51–52. In ‘Roadmap on STIRAP applications’ by Bergmann, K.; Nägerl, H. C.; Panda, C.; Gabrielse, G.; Miloglyadov, E.; Quack, M.; Seyfang, G.; Wichmann, G.; Ospelkaus, S.; Kuhn, A.; Longhi, S.; Szameit, A.; Pirro, P.; Hillebrands, B.; Zhu, X. F.; Zhu, J.; Drewsen, M.; Hensinger, W. K.; Weidt, S.; Halfmann, T.; Wang, H. L.; Paraoanu, G. S.; Vitanov, N. V.; Mompart, J.; Busch, T.; Barnum, T. J.; Grimes, D. D.; Field, R. W.; Raizen, M. G.; Narevicius, E.; Auzinsh, M.; Budker, D.; Pálffy, A.; Keitel, C. H.; *J. Phys. B: At. Mol. Opt. Phys.*, **2019**, *52*, 202001 (55 pp.).
85. Quack, M. On the Measurement of CP-Violating Energy Differences in Matter-Antimatter Enantiomers. *Chem. Phys. Lett.* **1994**, *231*, 4–6.
86. Quack, M. Comments on Intramolecular Dynamics and Femtosecond Kinetics, Proc. 20th Solvay Conference “Chemical reactions and their control on the femtosecond time scale” *Adv. Chem. Phys.* **1997**, *101*, 83–84, 92–93, 202, 277–278, 282, 373–388, 443, 453–456, 459, 586–591, 595.
87. Luckhaus, D.; Quack, M.; Stohner, J. Femtosecond Quantum Structure, Equilibration and Time-Reversal for the CH-Chromophore Dynamics in CHD<sub>2</sub>F. *Chem. Phys. Lett.* **1993**, *212*(5), 434–443.
88. Quack, M. *Naturwissenschaft als Beruf und Abenteuer: Servir sans Disparâtre. Lecture ETH Zürich 2014*, <https://video.ethz.ch/speakers/lecture/7f8b9b8c-78e6-4051-9bf5-6f963118eaef.html>.

89. Quack, M.; Thöne, H. J. Absolute and Relative Rate Coefficients in the IR-Laser Chemistry of Bichromophoric Fluorobutanes – Tests for Intermolecular and Intramolecular Selectivity. *Chem. Phys. Lett.* **1987**, *135*(6), 487–494.
90. Quack, M.; Merkt, F., Eds.; *Handbook of High-Resolution Spectroscopy*; 3 volumes. Wiley: Chichester, New York, 2011.
91. Albert, S.; Keppler Albert, K.; Quack, M. High Resolution Fourier Transform Infrared Spectroscopy. In *Handbook of High Resolution Spectroscopy*; Quack, M., Merkt, F., Eds.; Vol. 2, Wiley: Chichester, New York, 2011; pp 965–1019. (Chapter 26).
92. Snels, M.; Horká-Zelenková, V.; Hollenstein, H.; Quack, M. High Resolution FTIR and Diode Laser Spectroscopy of Supersonic Jets. In *Handbook of High Resolution Spectroscopy*; Quack, M., Merkt, F., Eds.; Vol. 2, Wiley: Chichester, New York, 2011; pp 1021–1067. Chapter 27.
93. Hippler, M.; Miloglyadov, E.; Quack, M.; Seyfang, G. Mass and Isotope Selective Infrared Spectroscopy. In *Handbook of High Resolution Spectroscopy*; Quack, M., Merkt, F., Eds.; Vol. 2, Wiley: Chichester, New York, 2011; pp 1069–1118. (Chapter 28).
94. Bauder, A. Fundamentals of Rotational Spectroscopy. In *Handbook of High Resolution Spectroscopy*; Quack, M., Merkt, F., Eds.; Vol. 1, John Wiley & Sons, Ltd.: Chichester, UK, 2011; pp 57–116. (Chapter 2).
95. Wörner, H. J.; Merkt, F. Fundamentals of Electronic Spectroscopy. In *Handbook of High Resolution Spectroscopy*; Quack, M., Merkt, F., Eds.; Vol. 1, Wiley: Chichester, UK, 2011; pp 175–262. (Chapter 4).
96. Merkt, F.; Willitsch, S.; Hollenstein, U. High-resolution Photoelectron Spectroscopy. In *Handbook of High Resolution Spectroscopy*; Quack, M., Merkt, F., Eds.; Vol. 3, John Wiley & Sons, Ltd.: Chichester, UK, 2011; pp 1617–1654.
97. Cohen, E. R.; Cvitas, T.; Frey, J. G.; Holmström, B.; Kuchitsu, K.; Marquardt, R.; Mills, I.; Pavese, F.; Quack, M.; Stohner, J.; Strauss, H. L.; Takami, M.; Thor, A. J. *Quantities, Units and Symbols in Physical Chemistry*, 3rd ed.; IUPAC and Royal Society of Chemistry, RSC Publishing: Cambridge, 2007.
98. Bureau International des Poids et Mesures. *Le Système International d'Unités (SI)*, 9th ed.; BIPM: Sèvres, 2019.
99. Arias, E. F.; Petit, G. The Hyperfine Transition for the Definition of the Second. *Ann. Phys.* **2019**, *531*(5), 1900068.
100. Townes, C. H.; Schawlow, A. L. *Microwave Spectroscopy*. McGraw-Hill: New York, 1955.
101. Quack, M. Intramolekulare Dynamik: Irreversibilität, Zeitumkehrsymmetrie und eine absolute Moleküluhr. *Nova Acta Leopoldina* **1999**, *81*(Neue Folge (No. 314)), 137–173.
102. Staudacher, F. *Jost Bürgi, Kepler und der Kaiser: Uhrmacher, Instrumentenbauer, Astronom, Mathematiker, 1552–1632*. Verlag Neue Zürcher Zeitung: Zurich, 2013.
103. Marquardt, R.; Quack, M. Statistical Aspects of the Radiative Excitation of the Harmonic-Oscillator. *J. Phys. Chem.* **1994**, *98*(13), 3486–3491.
104. Marquardt, R.; Quack, M. Radiative Excitation of the Harmonic Oscillator With Applications to Stereomutation in Chiral Molecules. *Z. Phys. D Atoms Mol. Clusters* **1996**, *36*(3–4), 229–237.
105. Quack, M. Discussion Contributions on High Resolution Spectroscopy (on Local and Global Vibrational States). *Farad. Disc.* **1981**, *71*, 359–364.
106. Quack, M. On the Emergence of Simple Structures in Complex Phenomena: Concepts and Some Numerical Examples. *Adv. Chem. Phys.* **2014**, *157*, 97–116.
107. Quack, M.; Sutcliffe, E. On the Possibility of Mode-Selective IR-Multiphoton Excitation of Ozone. *Chem. Phys. Lett.* **1984**, *105*(2), 147–152.
108. Quack, M. Reaction Dynamics and Statistical Mechanics of the Preparation of Highly Excited States by Intense Infrared Radiation. In *Adv. Chem. Phys.*, Vol. 50; Lawley, K., Prigogine, I., Rice, S. A., Eds.; John Wiley & Sons: Chichester and New York, 1982; pp 395–473.
109. Hehenberger, M.; McIntosh, H. V.; Brändas, E. Weyl's Theory Applied to the Stark Effect in the Hydrogen Atom. *Phys. Rev. A* **1974**, *10*(5), 1494–1506.

110. Hohenberger, M.; Laskowski, B.; Brändas, E. Weyl's Theory Applied to Predissociation by Rotation. I. Mercury Hydride. *J. Chem. Phys.* **1976**, *65*(11), 4559–4570.
111. Moiseyev, N. *Non-Hermitian Quantum Mechanics*. Cambridge University Press: Cambridge, 2011.
112. Breit, G.; Wigner, E. Capture of Slow Neutrons. *Phys. Rev.* **1936**, *49*, 519–531.
113. Rittby, M.; Elander, N.; Brändas, E.; Barany, A. Resonance Structure in Charge Transfer Cross Sections: An Application to the  $\text{N}^{3+} + \text{H}$  to  $\text{N}^{2+} + \text{H}^+$  Reaction. *J. Phys. B At. Mol. Phys.* **1984**, *17*(20), L677–L681.
114. Quack, M.; Troe, J. Statistical Methods in Scattering. In *Theoretical Chemistry: Advances and Perspectives (Theory of Scattering, Papers in Honor of Henry Eyring)*; Henderson, D. Ed.; Vol. 6B, Academic Press: New York, 1981; pp 199–276.
115. Heisenberg, W. Über den anschaulichen Inhalt der quantentheoretischen Kinematik und Mechanik. *Z. Phys.* **1927**, *43*, 172–198.
116. Pauli, W. Die allgemeinen Prinzipien der Wellenmechanik. In *Handbuch der Physik*, 2. Auflage; Geiger, H., Scheel, K., Bethe, H., Hund, F., Mott, N. F., Pauli, W., ... Redaktor, A. S., Eds.; Springer Verlag: Berlin Heidelberg, 1933; pp 83–272. (Chapter 2).
117. Pauli, W. Die allgemeinen Prinzipien der Wellenmechanik. In *Encyclopedia of Physics*; Flügge, S. Ed.; Vol. 5 Part 1, Springer Verlag, 1958; pp 1–168. Berlin, Göttingen, Heidelberg, (notably footnote, page 60) Vol.
118. Aharonov, Y.; Bohm, D. Time in the Quantum Theory and the Uncertainty Relation for Time and Energy. *Phys. Rev.* **1961**, *122*, 1649–1658. <https://doi.org/10.1103/PhysRev.122.1649>.
119. Kobe, D. H.; Aguilera-Navarro, V. C. Derivation of the Energy-Time Uncertainty Relation. *Phys. Rev. A* **1994**, *50*(2), 933–938. <https://doi.org/10.1103/PhysRevA.50.933>.
120. Pfeifer, P.; Fröhlich, J. Generalized Time–Energy Uncertainty Relations and Bounds on Lifetimes of Resonances. *Rev. Mod. Phys.* **1995**, *67*(4), 759–779. <https://doi.org/10.1103/RevModPhys.67.759>.
121. Hilgevoord, J. The Uncertainty Principle for Energy and Time. *Am. J. Phys.* **1996**, *64*(12), 1451–1456. <https://doi.org/10.1119/1.18410>.
122. Briggs, J. S. A Derivation of the Time–Energy Uncertainty Relation. *J. Phys. Conf. Ser.* **2008**, *99*, 1–6, 0.1088/1742-6596/99/012002.
123. Dodonov, V. V.; Dodonov, A. V. Energy–Time and Frequency–Time Uncertainty Relations: Exact Inequalities. *Phys. Scr.* **2015**, *90*(7), 074049–1–22. <https://doi.org/10.1088/0031-8949/90/7/074049>.
124. Brändas, E. A Simple Communication Hypothesis: The Process of Evolution Reconsidered. In *Concepts, Methods and Applications of Quantum Systems in Chemistry and Physics. Progress in Theoretical Chemistry and Physics*; Wang, Y. A., Thachuk, M., Krems, R., Maruani, J., Eds.; Vol. 31, Springer: Berlin, 2018; pp 381–404.
125. Sakurai, J. J. *Modern Quantum Mechanics*. Benjamin/Cummings Publ. Menlo Park, CA, 1985.
126. Cohen-Tannoudji, C.; Diu, B.; Laloë, F. *Mécanique Quantique*. Hermann: Paris, 1973; 2 volumes.
127. Marquardt, R. A Formula for the Contribution of a Resonance to the Canonical Partition Function. *Mol. Phys.* **2019**, *117*(15–16), 1964–1970. <https://doi.org/10.1080/00268976.2018.1562578>.
128. Schopper, H.; Dilella, L. *60 years of CERN: Experiments and Discoveries*. World Scientific Publ: Singapore, 2015.
129. Schopper, H. Lebenszeiten im Mikrokosmos von ultrakurzen bis zu unendlichen und oszillierenden. In *Nova Acta Leopoldina NF 81, Nr. 314*; Köhler, W. Ed.; Wissenschaftliche Verlagsgesellschaft: Stuttgart, 1999; pp 109–134.

130. Quack, M. Electroweak Quantum Chemistry and the Dynamics of Parity Violation in Chiral Molecules. In *Modelling Molecular Structure and Reactivity in Biological Systems*, Proc. 7th WATOC Congress, Cape Town January 2005, Naidoo, K. J., Brady, J., Field, M. J., Gao, J., Hann, M., Eds.; Royal Soc. Chem: Cambridge, 2006; pp 3–38.
131. Quack, M.; Stohner, J.; Willeke, M. High-Resolution Spectroscopic Studies and Theory of Parity Violation in Chiral Molecules. *Ann. Rev. Phys. Chem.* **2008**, *59*, 741–769.
132. Fermi, E. Über den Ramaneffekt des Kohlendioxyds. *Z. Phys.* **1931**, *71*, 250–259.
133. Herzberg, G. *Molecular Spectra and Molecular Structure; II. Infrared and Raman Spectra of Polyatomic Molecules*. van Nostrand Company, Inc: Princeton, New Jersey, NY, 1945.
134. Quack, M.; Kutzelnigg, W. Molecular Spectroscopy and Molecular Dynamics—Theory and Experiment. *Ber. Bunsenges. Phys. Chem.* **1995**, *99*(3), 231–245.
135. Quack, M. Multiphoton Excitation. In *Encyclopedia of Computational Chemistry*; von Ragué Schleyer, P., Allinger, N., Clark, T., Gasteiger, J., Kollman, P. A., Schaefer, H. F., Schreiner, P. R., Eds.; Vol. 3, John Wiley & Sons, Ltd: Chichester, 1998; pp 1775–1791.
136. Quack, M. Theory of Unimolecular Reactions Induced by Monochromatic Infrared Radiation. *J. Chem. Phys.* **1978**, *69*(3), 1282–1307.
137. Marquardt, R.; Quack, M.; Stohner, J.; Thanopulos, I. Quantum Dynamics and Spectra of the Iodine Atom in a Strong Laser Field as Calculated With the URIMIR Package. *Mol. Phys.* **2019**, *117*, 3132–3147 (with 537 Pages of Supplementary Material Including URIMIR Package FORTRAN Code).
138. Yi, P. N.; Ozier, I.; Ramsey, N. F. Low-Field Hyperfine Spectrum of CH<sub>4</sub>. *J. Chem. Phys.* **1971**, *55*(11), 5215–5227. <https://doi.org/10.1063/1.1675660>.
139. Bordé, J.; Bordé, C. J.; Salomon, C.; Van Lerberghe, A.; Ouhayoun, M.; Cantrell, C. D. Breakdown of the Point-Group Symmetry of Vibration-Rotation States and Optical Observation of Ground-State Octahedral Splittings of <sup>32</sup>SF<sub>6</sub> Using Saturation Spectroscopy. *Phys. Rev. Lett.* **1980**, *45*(1), 14–17. <https://doi.org/10.1103/PhysRevLett.45.14>.
140. Kanamori, H.; Dehghani, Z. T.; Mizoguchi, A.; Endo, Y. Detection of Microwave Transitions between Ortho and Para States in a Free Isolated Molecule. *Phys. Rev. Lett.* **2017**, *119*(17), 173401. <https://doi.org/10.1103/PhysRevLett.119.173401>.
141. Pique, J. P.; Hartmann, F.; Bacis, R.; Churassy, S.; Koffend, J. B. Hyperfine-Induced Ungerade-Gerade Symmetry Breaking in a Homonuclear Diatomic Molecule near a Dissociation Limit: <sup>127</sup>I<sub>2</sub> at the <sup>2</sup>P<sub>3/2</sub>–<sup>2</sup>P<sub>1/2</sub> Limit. *Phys. Rev. Lett.* **1984**, *52*(4), 267–270. <https://doi.org/10.1103/PhysRevLett.52.267>.
142. Critchley, A. D. J.; Hughes, A. N.; McNab, I. R. Direct Measurement of a Pure Rotation Transition in H<sub>2</sub><sup>+</sup>. *Phys. Rev. Lett.* **2001**, *86*(9), 1725–1728. <https://doi.org/10.1103/PhysRevLett.86.1725>.
143. Critchley, A. D. J.; Hughes, A. N.; McNab, I. R.; Moss, R. E. Energy Shifts and Forbidden Transitions in H<sub>2</sub><sup>+</sup> Due to Electronic g/u Symmetry Breaking. *Mol. Phys.* **2003**, *101*(4–5), 651–661. <https://doi.org/10.1080/0026897021000021886>.
144. Tanaka, K.; Hayashi, M.; Ohtsuki, M.; Harada, K.; Tanaka, T. Millimetre-Wave Spectroscopy of Deuterated Vinyl Radicals, Observation of the Ortho-Para Mixing Interaction and Prediction of Fast Ortho-Para Conversion Rates. *Mol. Phys.* **2010**, *108*(18), 2289–2301. <https://doi.org/10.1080/00268971003685764>.
145. Dübal, H. R.; Quack, M.; Schmitt, U. High-Resolution Interferometric Infrared-Spectroscopy of CO<sub>2</sub> and CH<sub>4</sub> Vapor at Low-Temperatures near 10 K – Collisional Cooling in Supersonic Jets and Nuclear Spin Symmetry Conservation. *Chimia* **1984**, *38*(12), 438–439.
146. Amrein, A.; Quack, M.; Schmitt, U. High-Resolution Interferometric Fourier Transform Infrared Absorption Spectroscopy in Supersonic Free Jet Expansions: Carbon Monoxide, Nitric Oxide, Methane, Ethyne, Propyne, and Trifluoromethane. *J. Phys. Chem.* **1988**, *92*(19), 5455–5466.

147. Manca Tanner, C.; Quack, M. Reinvestigation of the  $\nu_2 + 2\nu_3$  Subband in the Overtone Icosad of  $^{12}\text{CH}_4$  Using Cavity Ring-Down (CRD) Spectroscopy of a Supersonic Jet Expansion. *Mol. Phys.* **2012**, *110*(17), 2111–2135.
148. Bjelobrk, Z.; Manca Tanner, C.; Quack, M. Investigation of the  $\nu_2 + 2\nu_3$  Subband in the Overtone Icosad of  $^{13}\text{CH}_4$  by Pulsed Supersonic Jet and Diode Laser Cavity Ring-Down Spectroscopy: Partial Rovibrational analysis and Nuclear Spin Symmetry Conservation. *Z. Phys. Chem.* **2015**, *229*, 1575–1607.
149. Manca Tanner, C.; Quack, M.; Schmidiger, D. Nuclear Spin Symmetry Conservation and Relaxation in Water ( $^1\text{H}_2^{16}\text{O}$ ) Studied by Cavity Ring-Down (CRD) Spectroscopy of Supersonic Jets. *J. Phys. Chem. A* **2013**, *117*(39), 10105–10118.
150. Manca Tanner, C.; Quack, M.; Schmidiger, D. Nuclear Spin Symmetry Conservation and Relaxation of Water ( $\text{H}_2\text{O}$ ) Seeded in Supersonic Jets of Argon and Oxygen: Measurements by Cavity Ring-Down Laser Spectroscopy. *Mol. Phys.* **2018**, *116*, 3718–3730.
151. Georges, R.; Michaut, X.; Moudens, A.; Goubet, M.; Pirali, O.; Soulard, P.; Asselin, P.; Huet, T.; Roy, P.; Fournier, M.; Vigasin, A. Nuclear Spin Symmetry Conservation in  $^1\text{H}_2^{16}\text{O}$  Investigated by Direct Absorption FTIR Spectroscopy of Water Vapor Cooled Down in Supersonic Expansion. *J. Phys. Chem. A* **2017**, *121*(40), 7455–7468. <https://doi.org/10.1021/acs.jpca.7b06858>.
152. Horká-Zelenková, V.; Seyfang, G.; Dietiker, P.; Quack, M. Nuclear Spin Symmetry Conservation Studied for Symmetric Top Molecules ( $\text{CH}_3\text{D}$ ,  $\text{CHD}_3$ ,  $\text{CH}_3\text{F}$ , and  $\text{CH}_3\text{Cl}$ ) in Supersonic Jet Expansions. *J. Phys. Chem. A* **2019**, *123*, 6160–6174.
153. Wichmann, G.; Miloglyadov, E.; Seyfang, G.; Quack, M. Nuclear Spin Symmetry Conservation Studied by Cavity Ring-Down Spectroscopy of Ammonia in a Seeded Supersonic Jet From a Pulsed Slit Nozzle. *Mol. Phys.* **2020**, *118*, e1752946 (25 pages).
154. Bonhoeffer, K. F.; Harteck, P. Experimente über Para- und Orthowasserstoff. *Naturwissenschaften* **1929**, *17*, 182.
155. Bonhoeffer, K. F.; Harteck, P. Para- und Ortho Wasserstoff. *Z. Phys. Chem. B* **1929**, *4*(1/2), 113–141.
156. Grohmann, T.; Manz, J. On the Impossibility of Localised States for Molecular Rotors With Cyclic Potentials. *Mol. Phys.* **2018**, *116*(19–20), 2538–2555.
157. Quack, M. Frontiers in Spectroscopy (Concluding paper to Faraday Discussion 150). *Farad. Disc.* **2011**, *150*, 533–565.
158. Quack, M. On the Fundamental and Approximate Symmetries in Molecular Quantum Dynamics and the Preparation of Exotic Superposition Isomers. In *Proc. Symp. MOLIM 2018—Molecules in Motion Athens*; Merkt, F., Quack, M., Thanopoulos, I., Vayenas, C. G., Eds.; 2018; p 36.
159. Beyer, M.; Hölsch, N.; Hussels, J.; Cheng, C. F.; Salumbides, E. J.; Eikema, K. S. E.; Ubachs, W.; Jungen, C.; Merkt, F. Determination of the Interval between the Ground States of Para- and Ortho- $\text{H}_2$ . *Phys. Rev. Lett.* **2019**, *123*(16), 163002. <https://doi.org/10.1103/PhysRevLett.123.163002>.
160. Ozier, I.; Yi, P. N.; Khosla, A.; Ramsey, N. F. Direct Observation of Ortho-Para Transitions in Methane. *Phys. Rev. Lett.* **1970**, *24*(12), 642–646.
161. Hougen, J. T. Interpretation of Molecular Beam Radio Frequency Ortho-Para Transitions in Methane. *J. Chem. Phys.* **1971**, *55*, 1122–1127.
162. Pepper, M. J. M.; Shavitt, I.; von Ragué Schleyer, P.; Glukhovtsev, M. N.; Janoschek, R.; Quack, M. Is the Stereomutation of Methane Possible? *J. Comp. Chem.* **1995**, *16*(2), 207–225.
163. Herzberg, G. *Molecular Spectra and Molecular Structure; III. Electronic Spectra of Polyatomic Molecules*. van Nostrand Company, Inc.: Princeton, New Jersey, New York, 1966
164. Longuet-Higgins, H. C. The Intersection of Potential Energy Surfaces in Polyatomic Molecules. *Proc. Roy. Soc. London A* **1975**, *344*(1637), 147–156.

165. Brändas, E.; Froelich, P. Level Crossings and Branch Points Studied by the Multidimensional Partitioning Technique. *Int. J. Quantum Chem.* **1978**, *13*(5), 619–626.
166. Albert, S.; Chen, Z.; Fábi, C.; Lerch, P.; Prentner, R.; Quack, M. A combined Gigahertz and Terahertz (FTIR) Spectroscopic Investigation of Meta-D-Phenol: Observation of Tunnelling Switching. *Mol. Phys.* **2016**, *114*(19), 2751–2768.
167. Albert, S.; Lerch, P.; Prentner, R.; Quack, M. Tunneling and Tunneling Switching Dynamics in Phenol and Its Isotopomers From High-Resolution FTIR Spectroscopy With Synchrotron Radiation. *Angew. Chem. Int. Edit.* **2013**, *52*(1), 346–349.
168. Fábi, C.; Albert, S.; Chen, Z.; Prentner, R.; Quack, M. A Molecular Quantum Switch Based on Tunneling in Meta-D-Phenol  $C_6H_4DOH$ . *Phys. Chem. Chem. Phys.* **2018**, *20*, 7387–7394.
169. Quack, M.; Willeke, M. Stereomutation Tunneling Switching Dynamics and Parity Violation in Chlorineperoxide Cl-O-O-Cl. *J. Phys. Chem. A* **2006**, *110*(9), 3338–3348.
170. Quack, M. The Concept of Law and Models in Chemistry. *Europ. Rev.* **2014**, *22*, S50–S86.
171. Nielsen, M. A.; Chuang, I. L. *Quantum Computation and Quantum Information*. Cambridge University Press, 2000.
172. Feringa, B. L.; Browne, W. R. *Molecular Switches*. Wiley-VCH, Weinheim, 2000.
173. Quack, M.; Schwarz, R.; Seyfang, G. Time-Resolved Infrared-Spectroscopic Observation of Relaxation and Reaction Processes During and After Infrared-Multiphoton Excitation of  $^{12}CF_3$  and  $^{13}CF_3$  With Shaped Nanosecond Pulses. *J. Chem. Phys.* **1992**, *96*(12), 8727–8740.
174. He, Y. B.; Pochert, J.; Quack, M.; Ranz, R.; Seyfang, G. Dynamics of Unimolecular Reactions Induced by Monochromatic IR Radiation: Experiment and Theory for  $C_nF_mH_kI \rightarrow C_nF_mH_k + I$  Probed With Hyperfine-, Doppler- and Uncertainty-Limited Time Resolution of Iodine-Atom IR Absorption. *Farad. Disc.* **1995**, *102*, 275–300.
175. Quack, M. Special Evening Lecture on the Superposition of the Enantiomers of Chiral Molecules, at 'Workshops on Molecular Structure, Rigidity, on Energy Surfaces and on Energy Scrambling in a Molecule: Now Stationary are Internal States, Bielefeld University and ZIF 1980, (unpublished, cited in Ref. 176 as 'Quack's experiment') and in part contained in Ref. 46, 47.
176. Pfeifer, P. Molecular Structure Derived From First-Principles Quantum Mechanics. Two Examples. In *Energy Storage and Redistribution in Molecules (Proc. 2 workshops, Bielefeld 1980)*; Hinze, J. Ed.; Plenum Press, 1983; pp 315–326.
177. Bakasov, A.; Ha, T. K.; Quack, M. Ab Initio Calculation of Molecular Energies Including Parity Violating Interactions. In *Chemical Evolution, Physics of the Origin and Evolution of Life, Proc. of the 4th Trieste Conference (1995)*; Chela-Flores, J., Raulin, F., Eds.; Kluwer Academic Publishers: Dordrecht, 1996; pp 287–296.
178. Quack, M.; Stohner, J. Parity Violation in Chiral Molecules. *Chimia* **2005**, *59*(7–8), 530–538 (Erratum for printer's errors: Chimia, 59, 712–712 (2005)).
179. Quack, M. How Important Is Parity Violation for Molecular and Biomolecular Chirality? *Angew. Chem. Int. Edit.* **2002**, *41*, 4618–4630, *Angew. Chem.* **2002**, *114*, 4812–4825 (2002).
180. Daussy, C.; Marrel, T.; Amy-Klein, A.; Nguyen, C. T.; Bordé, C. J.; Chardonnet, C. Limit on the Parity Nonconserving Energy Difference Between the Enantiomers of a Chiral Molecule by Laser Spectroscopy. *Phys. Rev. Lett.* **1999**, *83*, 1554–1557.
181. Tokunaga, S. K.; Stoefler, C.; Auguste, F.; Shelkovnikov, A.; Daussy, C.; Amy-Klein, A.; Chardonnet, C.; Darquié, B. Probing Weak Force-Induced Parity Violation by High-Resolution Mid-Infrared Molecular Spectroscopy. *Mol. Phys.* **2013**, *111*(14–15), 2363–2373.
182. Letokhov, V. S. On Difference of Energy Levels of Left and Right Molecules Due to Weak Interactions. *Phys. Lett. A* **1975**, *53*(4), 275–276.

183. Bauder, A.; Beil, A.; Luckhaus, D.; Müller, F.; Quack, M. Combined High Resolution Infrared and Microwave Study of Bromochlorofluoromethane. *J. Chem. Phys.* **1997**, *106*(18), 7558–7570.
184. Albert, S.; Bolotova, I.; Chen, Z.; Fábris, C.; Horný, L.; Quack, M.; Seyfang, G.; Zindel, D. High Resolution GHz and THz (FTIR) Spectroscopy and Theory of Parity Violation and Tunneling for 1,2-Dithiine ( $C_4H_4S_2$ ) as a Candidate for Measuring the Parity Violating Energy Difference Between Enantiomers of Chiral Molecules. *Phys. Chem. Chem. Phys.* **2016**, *18*(31), 21976–21993.
185. Albert, S.; Arn, F.; Bolotova, I.; Chen, Z.; Fábris, C.; Grassi, G.; Lerch, P.; Quack, M.; Seyfang, G.; Wokaun, A.; Zindel, D. Synchrotron-Based Highest Resolution Terahertz Spectroscopy of the  $\nu_{24}$  Band System of 1,2-Dithiine ( $C_4H_4S_2$ ): A Candidate for Measuring the Parity Violating Energy Difference between Enantiomers of Chiral Molecules. *J. Phys. Chem. Lett.* **2016**, *7*, 3847–3853.
186. Albert, S.; Bolotova, I.; Chen, Z.; Fabri, C.; Quack, M.; Seyfang, G.; Zindel, D. High-Resolution FTIR Spectroscopy of Trisulfane HSSH: A Candidate for Detecting Parity Violation in Chiral Molecules. *Phys. Chem. Chem. Phys.* **2017**, *19*(19), 11738–11743.
187. Dunitz, J. D. *X-ray Analysis and the Structure of Organic Molecules*. Cornell University Press: Ithaca, 1979.
188. Shechtman, D. Quasi-Periodic Materials—A Paradigm Shift in Crystallography, Lecture at the Annual Symposium ‘Symmetry and Asymmetry in Science and Art’, Halle, Saale. In *Nova Acta Leopoldina NF* **127**, *2019*, Supplementum No 34; Quack, M., Hacker, J., Eds.; 2015; pp 11–36 (preface by the editors pp 7–10).
189. Berger, R. Parity-violation effects in molecules. In *Relativistic Electronic Structure Theory. Part 2 (Applications)*; Schwerdtfeger, P. Ed.; Elsevier: Amsterdam, 2004.
190. Berger, R.; Stohner, J. Parity Violation. *WIREs Comp. Mol. Sci.* **2019**, *9*(3), e1396.
191. Horný, L.; Quack, M. Computation of Molecular Parity Violation Using the Coupled-Cluster Linear Response Approach. *Mol. Phys.* **2015**, *113*(13–14), 1768–1779.
192. Lee, T. D.; Yang, C. N. Question of Parity Conservation in Weak Interactions. *Phys. Rev.* **1956**, *104*, 254–258.
193. Wu, C. S.; Ambler, E.; Hayward, R. W.; Hopps, D. D.; Hudson, R. P. Experimental Test of Parity Conservation in Beta Decay. *Phys. Rev.* **1957**, *105*, 1413–1415.
194. Schopper, H. Circular Polarization of Gamma-Rays – Further Proof for Parity Failure in Beta-Decay. *Phil. Mag.* **1957**, *2*, 710–713.
195. Schopper, H. Die Elastische Streuung von Gamma-Strahlen bei kleinen Streuwinkeln. *Z. Phys.* **1957**, *147*, 253–260.
196. Garwin, R. L.; Lederman, L. M.; Weinrich, M. Observation of the Failure of Conservation of Parity and Charge Conjugation in Meson Decays—The Magnetic Moment of the Free Muon. *Phys. Rev.* **1957**, *105*, 1415–1417.
197. Friedman, J. I.; Telegdi, V. L. Nuclear Emulsion Evidence for Parity Nonconservation in the Decay Chain  $\pi^+ - \mu^+ - \epsilon^+$ . *Phys. Rev.* **1957**, *105*, 1681–1682.
198. Hegström, R.; Rein, D. W.; Sandars, P. G. H. Calculation of Parity Non-Conserving Energy Difference Between Mirror-Image Molecules. *J. Chem. Phys.* **1980**, *73*, 2329–2341.
199. Mason, S. F.; Tranter, G. E. The Parity-Violating Energy Difference Between Enantiomeric Molecules. *Mol. Phys.* **1984**, *53*, 1091–1111.
200. Kikuchi, O.; Wang, H. Parity-Violating Energy Shift of Glycine, Alanine, and Serine in the Zwitterionic Forms. *Bull. Chem. Soc. Jpn.* **1990**, *63*, 2751–2754.
201. Wiesenfeld, L. Effect of Atomic Number on Parity-Violating Energy Differences Between Enantiomers. *Mol. Phys.* **1988**, *64*(4), 739–745.
202. Lazzaretti, P.; Zanasi, R. On the Calculation of Parity-Violating Energies in Hydrogen Peroxide and Hydrogen Disulphide Molecules Within the Random-Phase Approximation. *Chem. Phys. Lett.* **1997**, *279*, 349–354.

203. Laerdahl, J. K.; Schwerdtfeger, P. Fully Relativistic Ab Initio Calculations of the Energies of Chiral Molecules Including Parity-Violating Weak Interactions. *Phys. Rev. A* **1999**, *60*, 4439–4453.
204. Hennum, A. C.; Helgaker, T.; Klopper, W. Parity-Violating Interaction in  $\text{H}_2\text{O}_2$  Calculated From Density-Functional Theory. *Chem. Phys. Lett.* **2002**, *354*, 274–282.
205. Schwerdtfeger, P.; Saué, T.; van Stralen, J. N. P.; Visscher, L. Relativistic Second-Order Many-Body And Density-Functional Theory for the Parity-Violation Contribution to the C-F Stretching Mode in CHFCIBr. *Phys. Rev. A* **2005**, *71*, 012103.
206. Gabrielse, G. Probing Nature's Fundamental Symmetries. One Slow Particle at a Time. In *Symmetrie und Asymmetrie in Wissenschaft und Kunst, Nova Acta Leopoldina NF 127 Nr. 412*; Quack, M., Hacker, J., Eds.; Wissenschaftliche Verlagsgesellschaft: Stuttgart, 2016; pp 91–98.
207. Hudson, J. J.; Sauer, B. E.; Tarbutt, M. R.; Hinds, E. A. Measurement of the Electron Electric Dipole Moment Using YbF Molecules. *Phys. Rev. Lett.* **2002**, *89*(2), 023003.
208. Adler, R. CPLEAR collaboration. Direct Measurement of T Violation in the Neutral Kaon System Using Tagged  $\text{K}^0, \bar{\text{K}}^0$  at LEAR. In *Proceedings of the IV International Symposium on Weak and Electromagnetic Interactions*; Nuclei, Ejiri, H., Kishimoto, T., Salo, T., Eds.; World Scientific: Singapore, 1995; pp 53–57.
209. The ALPHA Collaboration (Amaldi et al.) Investigation of the Fine Structure of Antihydrogen. *Nature* **2020**, *578*, 375–380.
210. Dehmelt, H. *Experiments With an Isolated Subatomic Particle at Rest*. The Nobel foundation: Stockholm, 1989.
211. Van Dyck, R. S.; Schwinberg, P. B.; Dehmelt, H. G. New High-Precision Comparison of Electron and Positron g Factors. *Phys. Rev. Lett.* **1987**, *59*(1), 26–29.
212. Dehmelt, H.; Middleman, R.; Van Dyck, R. S.; Schwinberg, P. Past Electron-Positron  $g - 2$  Experiments Yielded Sharpest Bound on CPT Violation for Point Particles. *Phys. Rev. Lett.* **1999**, *83*(23), 4694–4696.
213. Bloch, P. CPT Invariance Tests in Neutral Kaon Decay. *Eur. Phys. J. C* **2000**, *15*, 509–512 (part of particle data group review, *Eur. Phys. J. C* **2000**, *15*, 1, Bartels, J. R. ed.).
214. Quack, M. Molecular Infrared-Spectra and Molecular-Motion. *J. Mol. Struct.* **1995**, *347*, 245–266.
215. Boyle, L.; Finn, K.; Turok, N. CPT-Symmetric Universe. *Phys. Rev. Lett.* **2018**, *121*, 251301.
216. Ernst, R. R.; Carrington, T., Jr.; Seyfang, G.; Merkt, F. Editorial to the Special Issue of Molecular Physics. *Mol. Phys.* **2013**, *111*, 1939–1963.
217. Glänzer, K.; Quack, M.; Troe, J. High Temperature UV Absorption and Recombination of Methyl Radicals in Shock Waves. In *16th Symposium (International) on Combustion*, The Combustion Institute: Pittsburgh, 1977; pp 949–960.
218. Glänzer, K.; Quack, M.; Troe, J. A Spectroscopic Determination of the Methyl Radical Recombination Rate Constant in Shock Waves. *Chem. Phys. Lett.* **1976**, *39*, 304–309.
219. Couroul, A.; Manceau, M.; Pierens, M.; Lecordier, L.; Tran, D. B. A.; Santagata, R.; Argence, B.; Goncharov, A.; Lopez, O.; Abgrall, M.; Coq, Y. L.; Targat, R. L.; Martinez, H. A.; Lee, W. K.; Xu, D.; Pottie, P. E.; Hendricks, R. J.; Wall, T. E.; Bieniewska, J. M.; Sauer, B. E.; Tarbutt, M. R.; Amy-Klein, A.; Tokunaga, S. K.; Darquié, B. A New Experiment to Test Parity Symmetry in Cold Chiral Molecules Using Vibrational Spectroscopy. *Quantum Electron.* **2019**, *49*, 288–292.
220. Bohr, N. Das Quantenpostulat und die neuere Entwicklung der Atomistik. *Naturwissenschaften* **1928**, *16*, 245–257.
221. Fritzsch, H. Symmetrien der Physik. In *Symmetrie und Asymmetrie in Wissenschaft und Kunst, Nova Acta Leopoldina NF 127 Nr. 412*; Quack, M., Hacker, J., Eds.; Wissenschaftliche Verlagsgesellschaft: Stuttgart, 2016; pp 75–90.

222. Jenni, P. The Long Journey to the Higgs Boson and Beyond at the Large Hadron Collider (LHC). In *Symmetrie und Asymmetrie in Wissenschaft und Kunst, Nova Acta Leopoldina NF 127 Nr. 412*; Quack, M., Hacker, J., Eds.; Wissenschaftliche Verlagsgesellschaft: Stuttgart, 2016; pp 99–117.
223. Particle Data Group Review of Particle Physics. *Phys. Rev. D* **2018**, *98*, 030001.
224. Quadt, A. Top Quark Physics at Hadron Colliders. *Eur. Phys. J. C Part. Fields* **2006**, *48*, 848.
225. CMS Collaboration. Measurements of the Higgs Boson Width and Anomalous HVV Couplings From On-Shell and Off-Shell Production in the Four-Lepton Final State. *Phys. Rev. D* **2019**, *99*, 112003.
226. ATLAS Collaboration. Constraints on Off-Shell Higgs Boson Production and the Higgs Boson Total Width With the ATLAS Detector. *Phys. Lett. B* **2018**, *786*, 223–244.
227. Fritzsch, H. Dark Matter and Excited Weak Bosons. *Mod. Phys. Lett. A* **2017**, *32*, 1730009-1–5 (and private communication 2020).
228. Quack, M.; Stohner, J. Combined Multidimensional Anharmonic and Parity Violating Effects in CDBrClF. *J. Chem. Phys.* **2003**, *119*, 11228–11240.
229. Beil, A.; Luckhaus, D.; Marquardt, R.; Quack, M. Intramolecular Energy-Transfer and Vibrational Redistribution in Chiral Molecules—Experiment and Theory. *Faraday Discuss.* **1994**, *99*, 49–76.
230. Woodward, R. B.; Hoffmann, R. *The Conservation of Orbital Symmetry*. VCH Weinheim, 1970.
231. Mainzer, K. *Symmetries of Nature—A Handbook for Philosophy of Nature and Science*. De Gruyter: Berlin/New York, 1996.
232. Al-Shamery, K. *Moleküle aus dem All?* VCH Weinheim, 2011.
233. Yamagata, Y. A Hypothesis for the Asymmetric Appearance of Biomolecules on Earth. *J. Theor. Biol.* **1966**, *11*, 495–498.
234. Garay, A. S.; Hrasko, P. Neutral Currents in Weak Interactions and Molecular Asymmetry. *J. Mol. Evol.* **1975**, *6*, 77–89.
235. Harris, R.; Stodolsky, L. Quantum Beats in Optical Activity and Weak Interactions. *Phys. Lett. B* **1978**, *78*, 313–317.
236. Hänsch, T. W. *Passion for Precision, Nobel Lecture 2005*. The Nobel Foundation: Stockholm, 2006.
237. Zimmermann, C.; Hänsch, T. W. Antiwasserstoff: Die Schlüsseltechniken zur Erzeugung und Spektroskopie sind vorhanden. *Physik. Blätter* **1993**, *49*, 19–196.
238. Schwingenheuer, B.; Briere, R. A.; Barker, A. R.; Cheu, E.; Gibbons, L. K.; Harris, D. A.; Mako, G.; McFarland, K. S.; Roodman, A.; Wah, Y. W.; Winstein, B.; Winston, R.; Swallow, E. C.; Bock, G. J.; Coleman, R.; Crisler, M.; Enagonio, J.; Ford, R.; Hsiung, Y. B.; Jensen, D. A.; Ramberg, E.; Tschirhart, R.; Yamanaka, T.; Collins, E. M.; Gollin, G. D.; Gu, P.; Haas, P.; Hogan, W. P.; Kim, S. K.; Matthews, J. N.; Myung, S. S.; Schnetzer, S.; Somalwar, S. V.; Thomson, G. B.; Zou, Y. CPT Tests in the Neutral Kaon System. *Phys. Rev. Lett.* **1995**, *74*, 4376–4379.